The Propagation of
Low Frequency Sound
through an Audience

Von der Fakultät für Elektrotechnik und Informationstechnik der
Rheinischen-Westfälischen Technischen Hochschule Aachen
zur Erlangung des akademischen Grades einer

DOKTORIN DER NATURWISSENSCHAFTEN

genehmigte Dissertation

vorgelegt von

Diplom-Physikerin (Moscow State University)
Elena Shabalina

aus Ryazan, Russische Föderation

Berichter:

Universitätsprofessor Dr. rer. nat. Michael Vorländer
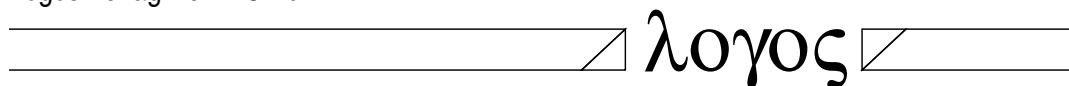Professor Dr. Christ Glorieux

Tag der mündlichen Prüfung: 30. April 2013

Diese Dissertation ist auf den Internetseiten der Hochschulbibliothek online verfügbar.

Elena Shabalina

The Propagation of Low Frequency Sound through an Audience

Aachener Beiträge zur Technischen Akustik

Contents

Abstract

In this thesis it is investigated, how low frequency sound (30-100Hz) propagates through an audience. At large outdoor concerts or festivals subwoofers, the dedicated low frequency loudspeakers, are often placed in a row in front of the stage as an evenly spaced array in order to control the directivity of sound at low frequencies. The audience itself often stands tightly packed in front of the array, so that sound waves propagate partly through the audience and partly over it. The purpose of the present research is to investigate how exactly the presence of the audience influences the propagation of sound. A new live measurement method was developed to evaluate the low frequency sound pressure level distribution without disturbing the ongoing event. It was experimentally shown that there is a measurable difference between the sound pressure level distribution in an empty venue and in the presence of an audience. The sound decay with the distance tends to be less in the presence of an audience. A mathematical model of an audience as a porous medium was constructed. This model allows to calculate the wave impedance of an audience from its concentration, the modelling results correspond to Boundary Element Method (BEM) modelling of an audience as a set of hard upright cylinders. It was shown both analytically and with the use of a BEM-simulation that the finite height of an audience leads to a modal field within the audience as well as evanescent waves. The study reaches the conclusion that at low frequencies an audience forms a medium with the impedance significantly different from the impedance of the air, which leads to the reflection of sound waves from the boundaries back into the audience and increase of the sound pressure level as well as interference effects. Possible applications of the findings are mainly sound system design and event planning.

1

Introduction

1.1 Motivation

The idea of studying the propagation of low frequency (20 - 120 Hz) sound through an audience comes from working on sound systems for large outdoor concerts and festivals. A lot of research is done on sound absorption by an audience in conventional concert halls, but modern large scale open air events require a slightly different approach. At these events subwoofers, the dedicated low frequency sound sources, are often placed in a row in front of the stage as an evenly spaced array (Fig. 1.1). This arrangement allows to control the directivity of low frequencies with simple beamforming, which provides an even sound pressure level distribution over the audience area. However, the audience itself often stands tightly packed in front of the array (Fig. 1.2), and sound waves therefore propagate partly through the crowd and partly over it, unlike concert halls where mid and HF sounds come mostly from above. The presence of the audience changes the sound pressure level distribution and the tonal balance of the sound system as a whole, but live sound engineers have different opinions about how exactly the tonal balance changes: some say that low frequencies become quieter in respect to mid- and high frequencies when the audience is present, some say exactly the opposite. So the purpose of the research was to find out, how in fact the audience influences the propagation of low frequencies, and to find a suitable mathematical model to describe this influence.

1.2 Outline of the thesis

The present thesis investigates the propagation of low frequency sound through an audience by means of direct live concert measurements, computer simulations,

Figure 1.1: An array of subwoofers in front of the stage

Figure 1.2: Tightly packed audience in front of a subwoofer array

an analytical solution of the wave equation and scale measurements. Chapter 1 contains the introduction, motivation and propositions. Chapter 2 presents an overview of similar effects or related topics in acoustics. Chapter 3 describes diffuse field measurements of sound absorption of the human body. Chapter 4 presents an analytical model of an audience as an equivalent fluid and uses the porous medium theory to estimate the acoustic impedance of the modelled audience with the concentration of people per square meter as a parameter. The influence of the finite height of the audience is considered as well. In Chapter 5 a Boundary Element Method simulation is used to evaluate the analytical predictions of Chapter 4, while in Chapter 6 the validity of the BEM-simulation results is tested by comparison with a scale model measurement. In Chapter 7 a newly

developed live measurement method and the results of concert measurements with and without audience are presented. In Chapter 8 the results are compared and discussed and Chapter 9 draws conclusions and gives an outline of future work.

The research resulted in the following findings, which are substantiated in the present thesis:

1. There is a measurable difference between sound pressure distribution in an empty venue and in the presence of an audience; sound often decays less when propagating through an audience than through air.

2. Energetic or diffuse field absorption of humans in the frequency range of 20-120 Hz is very small to negligible.

3. An audience can be modelled as equivalent fluid; the acoustic impedance of the fluid can be estimated using a porous medium model with the concentration of the audience as a parameter.

4. An audience forms a layer of finite height on a rigid surface, the sound field within the audience therefore has a modal structure, propagating and evanescent waves.

2

Literature and overview of similar or related effects

The influence of an audience on a sound field was mainly studied in room acoustics, where the absorption of the audience can significantly change the room's reverberation time and is therefore needed for a correct room acoustics prediction. Absorption coefficients of a seated audience were measured by Beranek in 1960 (BERANEK, 1960) and Kath and Kuhl (KATH and KUHL, 1964) in 1964, resulting in 0.37 at 67 Hz in the former and 0.1 under 100 Hz in the latter work. Later papers, such as (NISHIHARA, HIDAKA, and BERANEK, 2001), compare existing methods and results and come up with an average absorption value of 0.23 m^2 per person at 125 Hz.

Several authors dealt with sound propagation above the audience (ANDO and TAKAISHI, 1982; KUNSTMANN, 1967; KUTTRUFF, E. MEYER, and SCHULTE, 1965) and found that the diffraction on seat rows and listeners' heads causes dips in the frequency response.

However, these findings only take into account a regular distribution of listeners and therefore give no insight into sound propagation through a dense crowd.

Another topic possibly related to the subject of the present research is multiple scattering in random media. Listeners in the audience can be seen as a set of upright standing randomly distributed cylinders. Scattering on a single cylinder or sphere is described, for example, by (MECHEL, 1966) and (MORSE and INGARD, 1968). A fundamental theoretical work on the multiple scattering of waves was done by Foldy (FOLDY, 1945) and was motivated by his research on submarine detection and reflection of sound by bubbles created by a submarine's propeller. Foldy has calculated the configuration averages of wave function over a large ensemble of scatterers given the form of the wave function, distribution of

scatterers and scattering coefficients. The results are applicable to large number of scatterers with only a few scatterers per volume unit and predict absorption and partial scattering of the flux out of the average wave propagation direction. Foldy's procedure was generalized by Lax (LAX, 1951; LAX, 1952) and then followed by several publications of Twersky, whose research area was scattering theory of electro-magnetic waves. Twersky considered wave propagation through a region of randomly distributed scatterers, small (TWERSKY, 1962a) or large (TWERSKY, 1962b) in comparison to the wavelength, as well as multiple scattering by a distribution of parallel cylinders (TWERSKY, 1966).

An extensive overview over multiple scattering theories can be found in (ISHIMARU, 1999) and (MARTIN, 2006).

Recent applied research deals with sonic crystals (PEREZ-ARJONA and SANCHEZ-MORCILLO, 2006) and (PÉREZ-ARJONA et al., 2007): periodic acoustic media which allows nondiffractive propagation and localization of sound waves.

The attenuation of sound through trees seems relevant at first sight. Experimental results are presented by (PRICE, ATTENBOROUGH, and HEAP, 1988) along with theoretical considerations based on the theory of Embleton (EMBLETON, 1966). Both measurements and theory show additional attenuation of sound in comparison to the free field.

However, the studies mentioned above don't consider the relationships between wavelength, size of scatterers and distance between them, typical for an audience. Moreover, in a tightly packed audience back scattering might play an important role, and it is difficult to take into account. So, though multiple scattering theories could give an insight into microscopic effects of the sound propagation through an audience, a different approach has to be used.

Alternatively to multiple scattering models, a dense audience can be seen as a porous medium. People standing on a rigid surface form a rigid (or elastic) frame and the slots between people form pores. A lot of literature on porous materials is available, including fundamental works as (ZWIKKER and KOSTEN, 1949) and (MECHEL, 1989; MECHEL, 1995; MECHEL, 1998). Porous materials can have a rigid or elastic frame (where "frame" is the "skeleton" of the material); for different frames different models have to be used. A general approach is the so called equivalent fluid model: a porous medium is treated as a fluid, where the macroscopic properties are calculated from the microscopic structure of the

material. An overview of models for different kinds of microscopic structures of porous media is given in (ATTENBOROUGH, 1982). In the present thesis the simplest model of an audience as a set of upright hard cylinders is used, and the concentration, or number of cylinders per square meter, is taken as a parameter. The analytical model of Chapter 4 is based on the simplified description of the equivalent fluid model, given by (VRIES and BOONE, 2006).

3

Measurements of diffuse field absorption of the human body

In order to find a correct way to model the sound propagation through an audience, it is important to evaluate the energetic or diffuse field absorption of a single person. If the human body itself absorbs sound energy at low frequencies, it has to be taken into account in the model, resulting, for example, in a complex wave number in the equivalent fluid model. If the absorption is small or zero, it might be left out; in this case only the density of scatterers and the form of the crowd is important.

The frequency range of interest is from 30 Hz to 100 Hz. The sound absorption of the human body can be measured according to ISO 354 in a reverberation chamber. For the current work the total absorption per person is important, the area absorption coefficients were therefore not calculated. Previous works including (KATH and KUHL, 1964) or (E. MEYER, KUNSTMANN, and KUTTRUFF, 1964) present measurement results down to 100 Hz (KATH and KUHL, 1964) or 80 Hz. Below these frequencies a usual reverberation chamber is not big enough to create a diffuse field; also the lowest frequencies were not of the first interest for concert halls at the time the measurements were made. In the experiment described below, a larger reverberation chamber along with single mode evaluation technique was used to obtain the absorption characteristics of the human body at low frequencies.

3.1 Measurement setup

The measurements were conducted in a reverberation chamber of 217 m^3 volume and 220 m^2 surface area. A group of 20 students took part in the experiment

7

which allowed perform the measurement at three values of concentration of the audience: 3.8 pers./m^2, when people stand very close to each other, 1.5 pers./m^2 and 0.5 pers./m^2. To avoid the influence of the increase of sound pressure level close to the walls, the participants were asked to stay at least 0.5 m away from the walls. The measurement setup is shown in the Fig. 3.1.

The usual method to measure absorption or absorption coefficients is the diffuse field method according to the ISO 354. Impulse responses were measured using a sweep signal for three loudspeaker positions and four microphone positions for every concentration of the audience, which results in 12 impulse responses for every concentration. However, the Schroeder frequency of the reverberation chamber is about 163 Hz, so the frequency range of interest is in the range of strong modes (Fig. 3.2).

According to ISO 354, evaluation of the reverberation time and absorption should be done in 1/3 octave frequency bands which are relatively broad at low frequencies. To find out if the calculation in 1/3 octave bands still gives correct results, an alternative method was used to calculate the reverberation time and absorption of the audience: If modes don't overlap too much, the Q-factor of a single mode can be defined from its -3 dB level as shown in Fig. 3.3; the decay time can then be calculated as follows:

$$\ddot{x} + 2\gamma\dot{x} + \omega_0^2 x = 0 \tag{3.1}$$

$$Q = \frac{\omega_0}{2\gamma} = \frac{\omega_0}{\Delta\omega} \tag{3.2}$$

$$RT60 = -\frac{\ln 0.001}{\gamma} \tag{3.3}$$

Five single modes (24, 34, 38, 43 and 48 Hz) were picked in the lowest frequency range to compare with the calculation according to ISO 354. The Q-factor and the decay time were calculated for all the 12 measurements for each density and the empty room, then the average decay time was calculated for each mode, and from the difference in decay times for each mode in the empty and occupied room the absorption was calculated. The reverberation time of the empty room is shown on Fig. 3.4.

(a) Concentration 3.8 pers./m^2
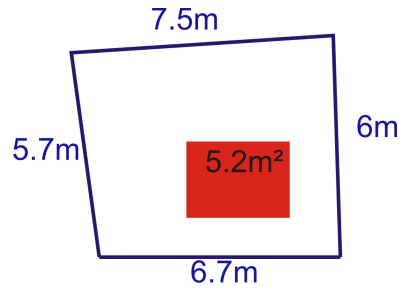
(b) Concentration 1.5 pers./m^2
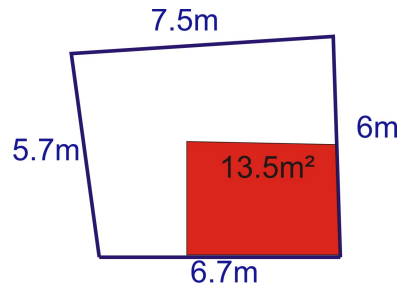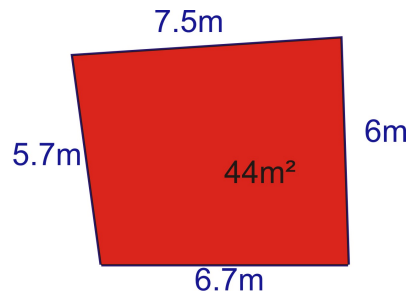

(c) Concentration 0.5 pers./m^2

Figure 3.1: Measurements setup: three different densities of the audience.
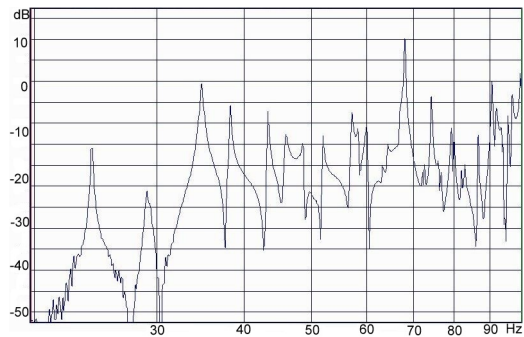
Figure 3.2: Frequency response of the reverberation chamber at low frequencies
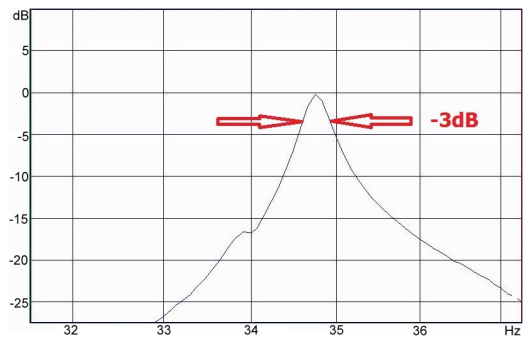

Figure 3.3: Modal decay time

3.2 Results

Absorption (per person) for different concentrations is shown in Fig. 3.5. The calculation using modal decay corresponds well with the calculation in 1/3 octave frequency bands according to ISO 354. The absorption for all three densities together is presented in Fig. 3.6. Table 3.1 represents the obtained values of the absorption per person.
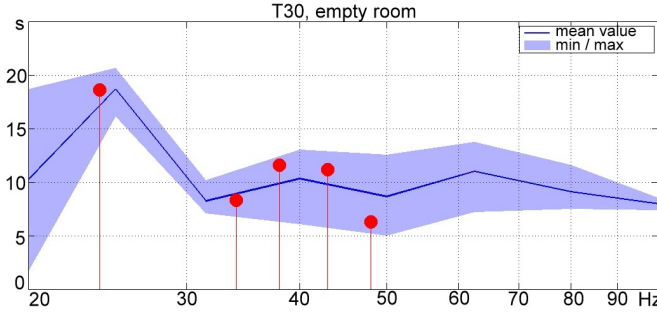
Figure 3.4: Reverberation time of the empty chamber. Blue line: calculated according to ISO 354, red dots: calculated from the modal decay

Density, $pers./m^2$	Frequency, Hz						
	31	40	50	63	80	90	100
3.8	0.05	0.03	0.03	0.05	0.06	0.06	0.05
1.5	0.04	0.04	0.05	0.04	0.06	0.05	0.05
0.5	0.03	0.05	0.06	0.05	0.06	0.07	0.07

Table 3.1: Absorption of human body, $m^2/pers.$

3.3 Discussion

The absorption measurements of the human body were conducted according to ISO 354 and evaluated both according to ISO 354 and using a modal calculation. The techniques give similar results in the frequency range from 30 Hz to 100 Hz. The values also don't contradict to those obtained by (E. MEYER, KUNSTMANN, and KUTTRUFF, 1964), (KATH and KUHL, 1964) in the overlapping frequency range of 80 Hz - 100 Hz.

With the characteristic absorption of 0.05 m^2 per person, an audience of 350 listeners (the amount that will be used for BEM-simulation and scale modelling) has a total absorption of 17.5 m^2 which results in an absorption coefficient of 0.06-0.1 for the corresponding listening area. The effect of the absorption is therefore considered small and is not taken into account in the analytical model, BEM-simulation and scale measurements. However, further investigations might improve the accuracy of the models by including the diffuse field absorption.

(a) Density 3.8 pers./m^2

(b) Density 1.5 pers./m^2
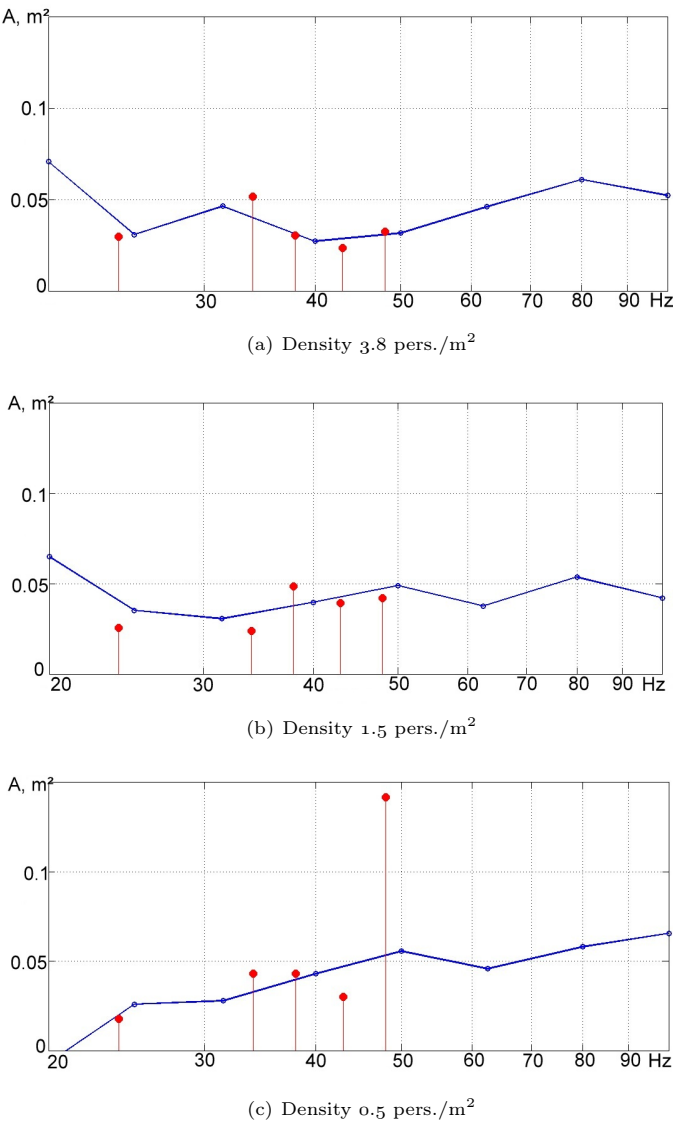

(c) Density 0.5 pers./m^2

Figure 3.5: Absorption per person for different densities of the audience. Blue line: calculated according to ISO 354, red dots: calculated from the modal decay
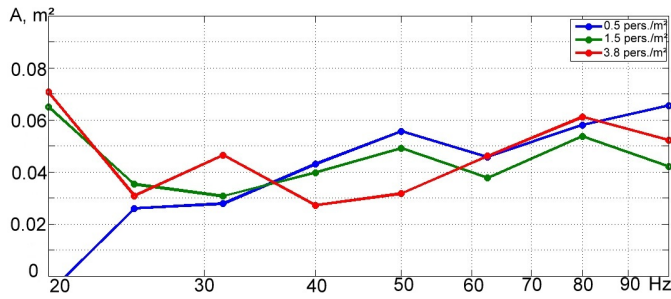
Figure 3.6: Absorption per person for the audience density of 0.5 pers./m^2 (blue), 1.5 pers./m^2 (green) and 3.8 pers./m^2 (red)

4

Analytical models

4.1 A one-dimensional model of an audience as a group of hard upright cylinders

One of the possible ways to describe the propagation of sound through an audience analytically is to represent the audience as a homogeneous medium with in general a complex speed of sound and complex density. The sound speed and the density of an audience should be calculated from its microscopic parameters such as the concentration of people and their average dimensions.

A simple way to construct such a medium is to represent people in an audience as infinitely long hard cylinders and consider it as a one-dimensional problem of plane wave propagation (Fig. 4.1).
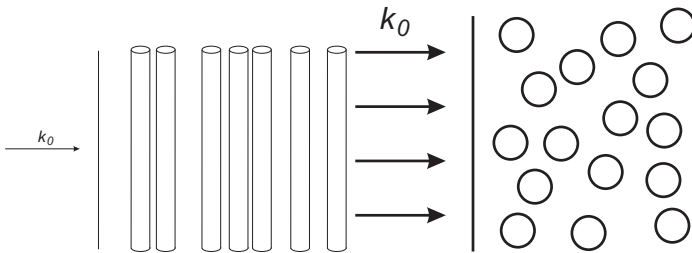

Figure 4.1: Plane wave propagation through a set of cylinders

This can be done according to the model of a porous medium with a rigid frame introduced by (ZWIKKER and KOSTEN, 1949) and described by (VRIES and BOONE, 2006). The model requires three parameters of the medium which can

be estimated from its structural parameters: porosity, structure factor and flow resistivity. The concentration of the crowd, or the number of persons per m^2 is taken as the known parameter, from which the other parameters are deduced.

As the first step the wave impedance of the medium is estimated.

For an audience modelled as a set of cylinders, "pores" are the spaces between the cylinders, and the cylinders form a rigid frame.

Porosity (h) is the ratio between the volume of air (V_{air})in the pores and the total volume (V_{total}) (eq. 4.1).

$$h = \frac{V_{air}}{V_{total}} \tag{4.1}$$

If cylinders are infinitely long, porosity is the ratio between the unoccupied area and the total area (eq. 4.2).

$$h = 1 - \nu\pi r^2, \tag{4.2}$$

where ν is the concentration of people in the audience and r is the average radius of the cylinders. The average radius of a human body is assumed 25 cm, which results in the maximum concentration value of $\nu < \frac{1}{\pi * r^2} = 5$. Reasonable values of ν range from 0 to 4.

The structure factor ξ is the ratio between the actual distance through the pores between two points, and the straight line between them (eq. 4.3).

$$\xi = 1 + \nu r(\pi - 2) \tag{4.3}$$

The flow resistivity (σ) takes into account the viscosity of air (ν) in the pores (eq. 4.4):

$$\sigma = \frac{\xi}{h} \frac{8\eta}{d^2}, \tag{4.4}$$

where $\eta = 1.85 * 10^{-5}$ is the viscosity of air and $d = \frac{1}{2\nu}$ the pore radius.

Then the wave number k in the medium can then be calculated (eq. 4.5)

$$k^2 = k_0^2 \sqrt{\xi - i\frac{\sigma h}{\omega \rho_0}}, \tag{4.5}$$

where $k_0 = \frac{\omega}{c_0}$ and $c_0 = \sqrt{\frac{\kappa p_0}{\rho_0}}$ are the wave number and the speed of sound in the air.

The wave number in the medium is generally complex (eq. 4.6 - 4.8):

$$k = k_p - i\alpha_\nu, \tag{4.6}$$

$$k_p = \frac{k_0}{\sqrt{2}} \sqrt{\xi + \sqrt{\xi^2 + \frac{\sigma^2 h^2}{\omega^2 \rho_0^2}}}, \tag{4.7}$$

$$\alpha_\nu = \frac{k_0}{\sqrt{2}} \sqrt{-\xi + \sqrt{\xi^2 + \frac{\sigma^2 h^2}{\omega^2 \rho_0^2}}} \tag{4.8}$$

The wave impedance (W) of the porous medium is given by (4.9)

$$W = \rho_\nu c_\nu \tag{4.9}$$

$$W = \rho_0 c_0 \frac{1}{h} \sqrt{\xi - i\frac{\sigma h}{\omega \rho_0}}, \tag{4.10}$$

where the effective density and the speed of sound are

$$\rho_\nu = \rho_0 \left(\frac{\xi}{h} - i\frac{\sigma}{\omega \rho_0} \right) \tag{4.11}$$

$$c_\nu = \frac{c_0}{\sqrt{\xi - i\frac{\sigma h}{\omega \rho_0}}} \tag{4.12}$$

The frequency dependent part of (4.10) is very small and can therefore be neglected. The real and imaginary parts of the relative wave impedance $W/\rho_0 c_0$ are presented in Fig. 4.2.
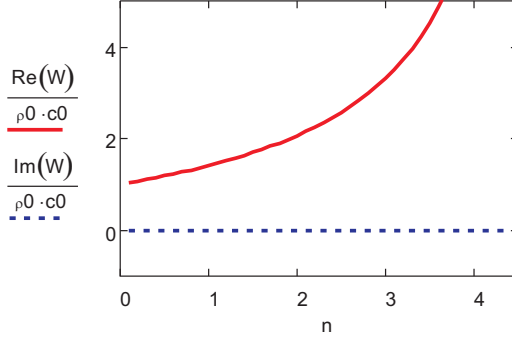

Figure 4.2: Real and imaginary parts of the relative wave impedance depending on the concentration

The imaginary part of the relative wave impedance is very close to zero for all concentrations, so it can be assumed real. The same is true for the speed of sound (4.12): it does not depend on frequency and the imaginary part is practically zero. The real part is decreasing with the increase of concentration (Fig. 4.3).
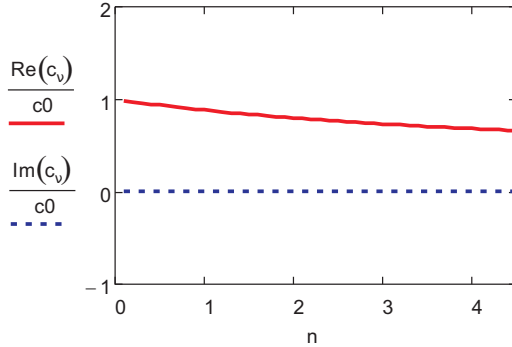

Figure 4.3: Real and imaginary parts of the speed of sound depending on the concentration

4.2 Waves in an audience of finite depth

Let's now consider a layer of a porous medium with a wave impedance W between two infinite layers of air (Fig. 4.4)
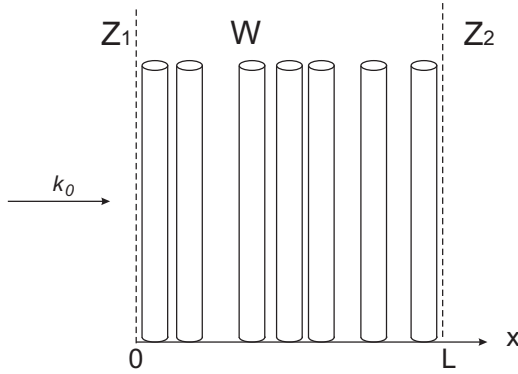
Figure 4.4: Plane wave propagation through a set of cylinders

The impedance of air is $Z_1 = Z_2 = Z = \rho_0 c_0$

The general solution of the wave equation (MORSE and INGARD, 1968) in every layer has a form of two plane waves travelling in opposite directions (eq. (4.14) - (4.18))

Layer of air 1:

$$p_1(x) = e^{i\omega t} \left[A_1 e^{-ik_0 x} + B_1 e^{ik_0 x} \right], \tag{4.13}$$

$$v_1(x) = e^{i\omega t} \left[\frac{A_1}{Z} e^{-ik_0 x} - \frac{B_1}{Z} e^{ik_0 x} \right] \tag{4.14}$$

Layer of the porous medium:

$$p(x) = e^{i\omega t} \left[A e^{-ikx} + B e^{ikx} \right], \tag{4.15}$$

$$v(x) = e^{i\omega t} \left[\frac{A}{W} e^{-ikx} - \frac{B}{W} e^{ikx} \right] \tag{4.16}$$

Layer of air 2:

$$p_2(x) = e^{i\omega t} \left[A_2 e^{-ik_0 x} + B_2 e^{ik_0 x} \right], \tag{4.17}$$

$$v_2(x) = e^{i\omega t} \left[\frac{A_2}{Z} e^{-ik_0 x} - \frac{B_2}{Z} e^{ik_0 x} \right] \tag{4.18}$$

The coefficients A, B, A_1, B_1, A_2, B_2 have to be found from the boundary conditions.

The boundary conditions are:

$$p_1(x = 0) = p(x = 0), \tag{4.19}$$
$$v_1(x = 0) = v(x = 0) \tag{4.20}$$

$$p_2(x = L) = p(x = L), \tag{4.21}$$
$$v_2(x = L) = v(x = L) \tag{4.22}$$

$$p_1(x = -\infty) = finite, \tag{4.23}$$
$$p_2(x = +\infty) = finite \tag{4.24}$$

From the boundary conditions (4.24) on infinity follows $A_1 = 0$ and $B_2 = 0$.

Applying the boundary conditions (4.20)-(4.24) on the general solutions (4.14)-(4.18) results in the values of the coefficients in terms of A (eq. (4.28))

$$A_1 = 0, \tag{4.25}$$
$$B_1 = -\frac{1 - \frac{Z}{W}}{1 + \frac{Z}{W}} A, \tag{4.26}$$
$$B = -\frac{1 - \frac{Z}{W}}{1 + \frac{Z}{W}} A, \tag{4.27}$$
$$A_2 = -\frac{2Z}{W} \frac{1}{1 - \frac{Z}{W}} A \tag{4.28}$$

The sound pressure within the layer of porous medium therefore is

$$p(x,t) = Ae^{i\omega t}\left[e^{-ikx} - \frac{1 - \frac{Z}{W}}{1 + \frac{Z}{W}}e^{ikx}\right] \tag{4.29}$$

Equation (4.29) can be written in the form

$$p(x,t) = Ae^{i\omega t}\left[e^{-ikx} + Re^{ikx}\right] \tag{4.30}$$

where

$$R = \frac{Z - W}{Z + W} \tag{4.31}$$

R can be seen as a reflection coefficient, real and imaginary parts of which are shown in Fig. 4.5.

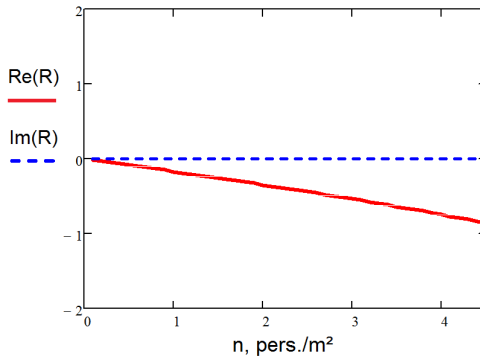**Figure 4.5:** Real and imaginary parts of the reflection coefficient depending on the concentration, frequency - 50 Hz.

Let's now consider the spatial distribution of the RMS sound pressure in the layer, which can be calculated as follows ((Möser, 2009)):

$$\tilde{p} = \sqrt{\frac{|p|^2}{2}} = \sqrt{\frac{p \cdot p^*}{2}} = \sqrt{\frac{1}{2}p_0^2(e^{-ikx} + Re^{ikx})(e^{ikx} + Re^{-ikx})} \tag{4.32}$$

Taking into account that the reflection coefficient is in general complex

$$R = re^{-ik\phi}, \qquad (4.33)$$

the RMS sound pressure is

$$\tilde{p} = \sqrt{\frac{p_0^2}{2}(e^{-ikx} + re^{i(kx+\phi)})(e^{ikx} + re^{-i(kx+\phi)})} = \sqrt{\frac{p_0^2}{2}[1 + 2rcos(2kx + \phi) + r^2]} \qquad (4.34)$$

The maxima occur at

$$x_{max} = \frac{\pi n - \phi}{2k}, n \in \mathbb{Z}, \qquad (4.35)$$

the maximum RMS sound pressure value is

$$\tilde{p}_{max} = \sqrt{\frac{p_0^2}{2}(1+r)^2}. \qquad (4.36)$$

The minima occur at

$$x_{min} = \frac{\pi(2n+1) - \phi}{2k}, n \in \mathbb{Z}, \qquad (4.37)$$

and the minimum RMS sound pressure value is

$$\tilde{p}_{min} = \sqrt{\frac{p_0^2}{2}(1-r)^2}. \qquad (4.38)$$

The distance between maxima and minima

$$\Delta x = \frac{\pi}{2k} = \frac{\pi c_\nu}{2\omega} \qquad (4.39)$$

depends on the wave number within the layer and, correspondingly, on the concentration of the audience. As the speed of sound within the layer c_ν decreases with the increase of concentration (Fig. 4.3), the distance between maxima also decreases. The difference between the maximum and minimum RMS sound pressure values depends on the reflection factor. At low concentrations (Fig.

4.5) the reflection factor is close to zero, so $\tilde{p}_{max} = \tilde{p}_{min} = \sqrt{\frac{p_0^2}{2}}$. As the concentration increases, the reflection factor and the maximum/minimum ratio increase (Fig. 4.6 and 4.7). With the increase of concentration the reflection coefficient approaches -1, which corresponds to a soft boundary condition. The amplitude of the corresponding standing wave at 50 Hz, shown in Fig. 4.7, represents a typical resonance with soft boundary conditions: the sound pressure is minimum at both boundaries, and the ratio between the extrema is maximal.
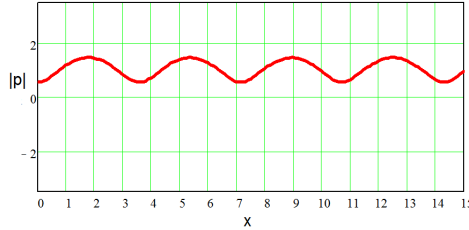

Figure 4.6: Amplitude of the standing wave caused by reflections from the boundaries of a layer of audience with maximum concentration of $\nu = 5pers./m^2$. $L = 15m$ is the thickness of the layer. Frequency - 50 Hz.

Figure 4.7: Amplitude of the standing wave caused by reflections from the boundaries of a layer of audience with maximum concentration of $\nu = 5pers./m^2$. $L = 15m$ is the thickness of the layer. Frequency - 50 Hz.
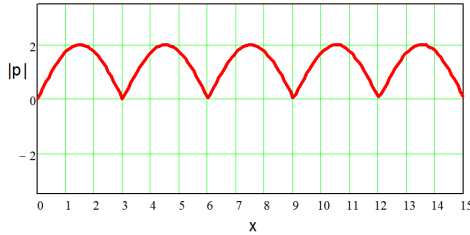
4.3 Audience with variable concentration

At real open-air festivals the concentration of the audience usually decreases with the distance to the stage. Let's consider the influence that the variable concentration might have on the reflection from the back of the audience.

At $x < 0$ the audience concentration is constant, at $0 < x < d$ it is decreasing from $\nu = \nu_0$ to $\nu = 0$ according to an arbitrary function $\nu = \nu(x)$, and at $x > d$ the concentration is zero.
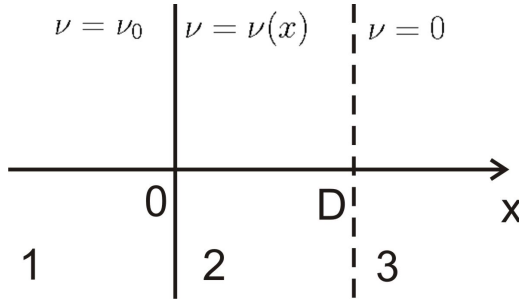
Figure 4.8: A one-dimensional model of an audience with variable concentration.

The parameters of the first layer can be calculated according to Section 4.1. The middle layer is a medium with variable parameters. If the concentration profile $\nu(x)$ is know, all medium parameters can be calculated according to Section 4.1. To describe the sound propagation through a medium with variable parameters, equations from Chapter 1 of (BREKHOVSKIKH and GODIN, 1989) are used.

For a time-harmonic wave in a static medium with variable parameters the Helmholtz equation takes the form:

$$\frac{\partial^2}{\partial x^2}\Psi + \left[k(x)^2 + \frac{1}{2\rho(x)}\frac{\partial^2 \rho(x)}{\partial x^2}\rho(x) - \frac{3}{4}\left(\frac{1}{\rho(x)}\frac{\partial \rho(x)}{\partial x}\right)^2 \right]\Psi = 0, \qquad (4.40)$$

where

$$\Psi(x) = \frac{p(x)}{\sqrt{\rho(x)}}, \qquad (4.41)$$

$$\mu(x) = k(x)^2 + \frac{1}{2\rho(x)}\frac{\partial^2 \rho(x)}{\partial x^2} - \frac{3}{4}\left(\frac{1}{\rho(x)}\frac{\partial \rho(x)}{\partial x}\right)^2 \qquad (4.42)$$

is an effective wave number within the layer, and

$$k(x) = \frac{\omega}{c(x)}. \qquad (4.43)$$

The solution of 4.40 has the form

$$\Psi(x) = A\left(e^{-i\mu(x)x} + Qe^{-i\mu(x)x}\right), \tag{4.44}$$

where A is the amplitude of a wave propagating from left to right and Q is the reflection factor from the boundary at $z = d$ ((SHVARTSBURG and EROKHIN, 1960)).

According to 4.41, the sound pressure excluding the time-harmonic component is

$$p(x) = \sqrt{\rho(x)}A\left(e^{-i\mu(x)x} + Qe^{-i\mu(x)x}\right). \tag{4.45}$$

The solutions of the corresponding wave equations for every layer along with their boundary conditions can be constructed similar to Section 4.2.

1. Layer of audience with constant concentration, $z < 0$:

$$p_1(x) = A_i\left(e^{-ik_\nu x} + Re^{ik_\nu x}\right) \tag{4.46}$$

2. Layer of audience with variable concentration, $0 < z < D$:

$$p_2(x) = \sqrt{\rho(x)}A\left(e^{-i\mu(x)x} + Qe^{i\mu(x)x}\right) \tag{4.47}$$

3. Layer of air, $z > D$:
$$p_3(x) = Be^{-ik_0 x}, \tag{4.48}$$

where A_i is the amplitude of the incident wave. The coefficients R, Q and B have to be found from the boundary conditions. The most interesting is R, the reflection coefficient from the layer of variable concentration back into the audience.

The boundary conditions are:

$x = 0$

$$A_i(1 + R) = \sqrt{\rho_\nu}A(1 + Q), \tag{4.49}$$

$$k_\nu A_i(1 - R) = \sqrt{\rho_\nu}\mu_\nu(1 - Q) \tag{4.50}$$

$x = D$

$$\sqrt{\rho_0}A\left(e^{-i\mu_0 D} + Qe^{i\mu_0 D}\right) = Be^{-ik_0 D}, \tag{4.51}$$

$$\mu_0\sqrt{\rho_0}A\left(e^{-i\mu_0 D} - Qe^{i\mu_0 D}\right) = k_0 Be^{-ik_0 D}, \tag{4.52}$$

where $\rho_\nu = \rho(0)$, $k_\nu = k(0)$, $\mu_\nu = \mu(0)$, $\rho_0 = \rho(D)$, $\mu_0 = \mu(D)$, and $k_0 = \frac{\omega}{c_0}$ is the wave number in air.

From the first two boundary conditions (4.49)-(4.50) R can be determined:

$$R = \frac{\left(1 - \frac{\mu_\nu}{k_\nu}\right) + Q\left(1 + \frac{\mu_\nu}{k_\nu}\right)}{\left(1 + \frac{\mu_\nu}{k_\nu}\right) + Q\left(1 - \frac{\mu_\nu}{k_\nu}\right)}, \tag{4.53}$$

where Q can be determined from the equations (4.51)-(4.52):

$$Q = \frac{1 - \frac{k_0}{\mu_0}}{1 + \frac{k_0}{\mu_0}}e^{-2i\mu_0 D}, \tag{4.54}$$

Inserting (4.54) into (4.53) gives

$$R = \frac{\left(1 - \frac{\mu_\nu}{k_\nu}\right) + \frac{1 - \frac{k_0}{\mu_0}}{1 + \frac{k_0}{\mu_0}}e^{-2i\mu_0 D}\left(1 + \frac{\mu_\nu}{k_\nu}\right)}{\left(1 + \frac{\mu_\nu}{k_\nu}\right) + \frac{1 - \frac{k_0}{\mu_0}}{1 + \frac{k_0}{\mu_0}}e^{-2i\mu_0 D}\left(1 - \frac{\mu_\nu}{k_\nu}\right)}, \tag{4.55}$$

At the right boundary of the variable concentration layer at $x = D$ the concentration approaches zero. To simplify the expression for the reflection coefficient R (4.55), the reflection coefficient from the right boundary Q can be roughly assumed zero: the concentration ν approaches zero and the medium on the left side of the boundary is arbitrary close to air. So, at the first rough approximation, we assume:

$$Q = 0 \tag{4.56}$$

In this case the simplified expression for R is

$$R = \frac{\left(1 - \frac{\mu_\nu}{k_\nu}\right)}{\left(1 + \frac{\mu_\nu}{k_\nu}\right)} \tag{4.57}$$

The results of this section can be verified by comparison to the the results of Section 4.4. If the length of the variable density layer D is infinitely small, the reflection coefficient (4.57) should be equal to the reflection coefficient (4.5).

The comparison is easy to conduct at the two extreme cases: $\nu_0 = 0$, which corresponds an air-air boundary, and $\nu_0 = max$, which corresponds to an abrupt transition from a maximum concentration to zero.

The reflection coefficient (4.57) for the case $\nu_0 = 0, D \to 0$ is shown in Fig. 4.9. As expected, the reflection coefficient from an air-air boundary is constant and equal to zero.
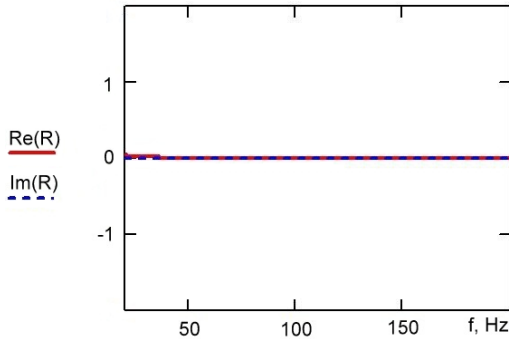

Figure 4.9: The reflection coefficient from a variable density layer according to (4.57), $\nu_0 = 0, D \to 0$.

Fig. 4.10 shows the reflection coefficient (4.57) for the case $\nu_0 = max, D \to 0$. It approaches -1, which corresponds to the result in Fig. 4.5 in Section 4.2.

Equation (4.40) allows to calculate the reflection coefficients for an arbitrary density profile and correspondingly arbitrary concentration profile $\nu = \nu(x)$. To illustrate the influence of the exact form of the profile on the reflection from the layer, two forms of profiles (4.59), (4.59) were calculated and are shown in the Fig. 4.11.
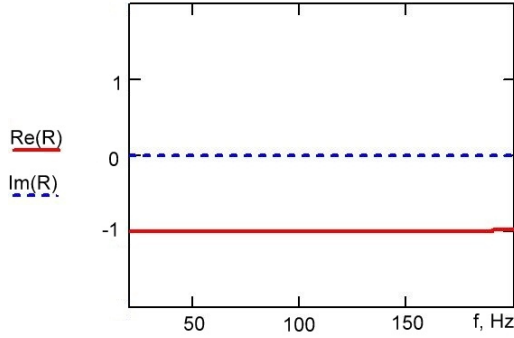
Figure 4.10: The reflection coefficient from a variable density layer according to (4.57), $\nu_0 = max, D \to 0$.

$$\nu(x) = \frac{\nu_0}{2}(cos(x\frac{\pi}{D}) + 1), \tag{4.58}$$

$$\nu(x) = -\frac{\nu_0}{D}x + \nu_0 \tag{4.59}$$

Fig. 4.11 shows the reflection coefficients for different depths D of the variable concentration layer. The best impedance match ($R = 0$) is achieved by the longest variable density layer ($D = 20m$), and the smallest D provides the strongest reflection. Also, the linear concentration profile provides a stronger reflection then the cosine-shaped profile.

Therefore, the exact way of how the concentration of people decreases towards the back of the audience influences the reflection of sound back into the audience from its rear boundary.

4.4 Waves in an infinite layer of an audience on a rigid floor

The one-dimensional model of an audience considered above assumes infinite height of cylinders. The wave propagation through an audience of a finite height will differ from the model, most likely, with the least error close to the ground and increasing error close the upper boundary. Another important effect of the finite height of an audience is that a layer of audience of finite height on a rigid
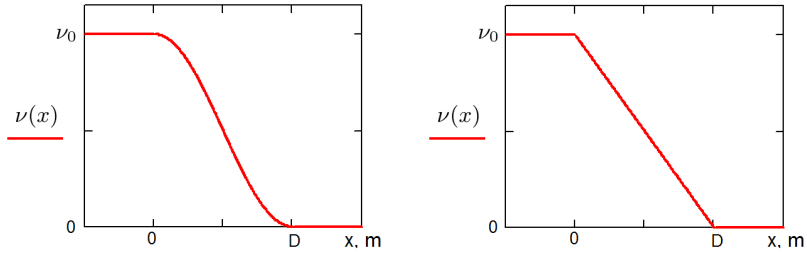
(a) Concentration profiles according to (4.59) (left) and (4.59) (right)
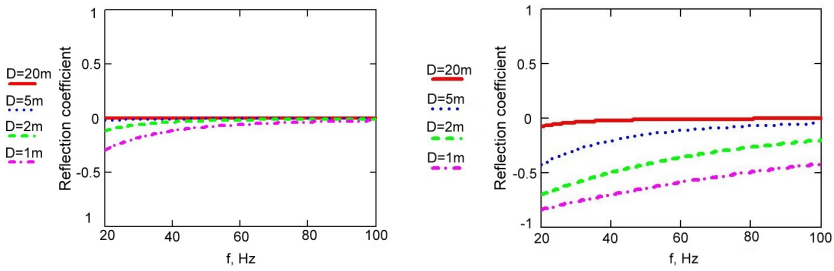
(b) Reflection coefficients for both profiles

Figure 4.11: Variable concentrations of an audience and corresponding reflection coefficients.

floor creates a kind of a waveguide. In this section the wave propagation in such a layer is considered.

The Helmholtz equation in cylindrical coordinates

Let's first consider the simplest case of an infinite layer of audience on a hard floor.

$$\nabla^2 p + k^2 p = 0 \tag{4.60}$$

Cylindrical coordinate system is chosen to allow a comparison to a BEM simulation in Section 5.2.3. The Helmholz equation in cylindrical coordinates:

$$\nabla^2 p = \frac{1}{r}\frac{\partial}{\partial r}\left(r\frac{\partial p}{\partial r}\right) + \frac{1}{r^2}\frac{\partial^2}{\partial \theta^2} + \frac{\partial^2}{\partial z^2} \tag{4.61}$$

Separation of variables:

$$p(r, \theta, z) = R(r)\Theta(\theta)Z(z) \tag{4.62}$$

Inserting (4.62) in (4.60) gives

$$\frac{d^2R}{dr^2}\Theta Z + \frac{1}{r}\frac{dR}{dr}\Theta Z + \frac{1}{r^2}\frac{d^2\Theta}{d\theta^2}RZ + \frac{d^2Z}{dz^2}R\Theta + k^2 R\Theta Z = 0$$

Multiplying by $\frac{r^2}{R\Theta Z}$ results in

$$\left[\frac{r^2}{R}\frac{d^2R}{dr^2} + \frac{r}{R}\frac{dR}{dr}\right] + \frac{1}{\Theta}\frac{d^2\Theta}{d\theta^2} + \frac{r^2}{Z}\frac{d^2Z}{dz^2} + k^2 r^2 = 0 \tag{4.63}$$

Now variables are separated. The equation for Θ is

$$\frac{1}{\Theta}\frac{d^2\Theta}{d\theta^2} = -m^2, \tag{4.64}$$

where a negative separation constant was chosen to provide a periodic solution. The general solution of (4.64) is

$$\Theta(\theta) = C_m \cos(m\theta) + D_m \sin(m\theta) \tag{4.65}$$

Inserting (4.64) back into (4.63) and dividing by r^2 gives

$$\frac{1}{R}\frac{d^2R}{dr^2} + \frac{1}{rR}\frac{dR}{dr} - \frac{m^2}{r^2} + \frac{1}{Z}\frac{d^2Z}{dz^2} + k^2 = 0 \tag{4.66}$$

The solution for $Z(z)$ must be periodical as well, so the differential equation also has a negative separation constant:

$$\frac{1}{Z}\frac{d^2Z}{dr^2} = -n^2 \tag{4.67}$$

Its general solution is

$$Z(z) = E_n e^{inz} + F_n e^{-inz} \tag{4.68}$$

By inserting (4.68) in (4.66) and multiplying by R gives

$$\frac{d^2R}{dr^2} + \frac{1}{r}\frac{dR}{dr} + \left(k^2 - n^2 - \frac{m^2}{r^2}\right)R = 0, \tag{4.69}$$

Which is a modified Bessel differential equation with a general travelling wave solution

$$R(r) = A_{mn}H_m^{(1)}(\sqrt{k^2 - n^2}r) + B_{mn}H_m^{(2)}(\sqrt{k^2 - n^2}r) \tag{4.70}$$

The general solution of the Helmholtz equation thus is

$$p(r, \theta, z) =$$

$$\sum_{m=0}^{\infty}\sum_{n=0}^{\infty}[A_{mn}H_m^{(1)}(\sqrt{k^2 - n^2}r) + B_{mn}H_m^{(2)}(\sqrt{k^2 - n^2}r)] \tag{4.71}$$

$$\times [C_m\cos(m\theta) + D_m\sin(m\theta)]\left[E_ne^{inz} + F_ne^{-inz}\right]$$

The coefficients A_{nm} will be defined by the sources inside the region, B_{nm} - by the outside sources since $H_m^{(1)}$ represents an outgoing wave and $H_m^{(2)}$ represents an ingoing wave (WILLIAMS, 1999).

Boundary conditions

The boundary conditions in the Z-direction are

$$\begin{cases} \frac{\partial p}{\partial z}|_{z=0} = 0 & - & \text{hard boundary,} \\ p(r, \theta, z)|_{z=H} = 0 & - & \text{soft boundary} \end{cases} \tag{4.72}$$

which for $Z(z)$ gives

$$\begin{cases} \frac{dZ}{dz}|_{z=0} = 0 \\ Z(z)|_{z=H} = 0 \end{cases} \tag{4.73}$$

For $E_ne^{inz} + F_ne^{-inz}$ the first boundary condition yields

$$inE_ne^{inz} - inF_ne^{-inz}|_{z=0} = 0 \qquad \text{and} \qquad E_n = F_n,$$

so

$$Z(z) = E_n \cos(nz),$$

after renaming $E_n \equiv 2E_n$.

The second boundary condition of (4.73) gives

$$Z(H) = E_n \cos(nH) = 0 \qquad \text{and} \qquad n = (l + \frac{1}{2})\frac{\pi}{H} \qquad \text{for all } l \in \mathbb{Z}, \, l \geq 0 \tag{4.74}$$

The expression for $Z(z)$ therefore is

$$Z(H) = E_l \cos((l + \frac{1}{2})\frac{\pi}{H}z) = 0 \qquad \text{for } l \in \mathbb{Z}, \, l > 0 \tag{4.75}$$

The general solution of the homogeneous Helmholtz equation in an infinite layer in cylindrical coordinates is

$$p(r, \theta, z) =$$

$$\sum_{m=0}^{\infty} \sum_{l=0}^{\infty} \left[A_{ml} H_m^{(1)} \left(\sqrt{k^2 - \left(l + \frac{1}{2}\right)^2 \frac{\pi^2}{H^2}} r \right) + B_{ml} H_m^{(2)} \left(\sqrt{k^2 - \left(l + \frac{1}{2}\right)^2 \frac{\pi^2}{H^2}} r \right) \right]$$

$$\times [C_m \cos(m\theta) + D_m \sin(m\theta)] \left[E_l \cos((l + \frac{1}{2})\frac{\pi}{H}z) \right] \tag{4.76}$$

where the coefficients $A_{ml}, B_{ml}, C_m, D_m, E_l$ depend on the source.

The last term of 4.76 represents vertical modes. The vertical mode index l defines a cutoff frequency for every vertical mode: the frequency that turns the expression under square root into negative and results in an evanescent wave ((4.77) and (4.78)).

$$k^2 - \left(l + \frac{1}{2}\right)^2 \frac{\pi^2}{H^2} > 0, \tag{4.77}$$

or

$$f_{cutoff} = c\frac{l + \frac{1}{2}}{2H}, \tag{4.78}$$

The angular mode index m defines the order of Hankel functions $H_m^{(1)}$ and $H_m^{(2)}$, where a higher order means a faster decay with the distance r.

Let's consider several examples of single modes in the layer. Fig. 4.12 shows the first two vertical modes and below them the first six modes in horizontal plane, calculated at a hight of 0.5m at 100Hz.

100Hz is above the cutoff frequency for the first vertical mode (Fig. 4.12), and below the cutoff frequency for the second vertical mode(right), so the second mode fades away faster. Higher orders of the Hankel function also provide a faster decay then low orders.
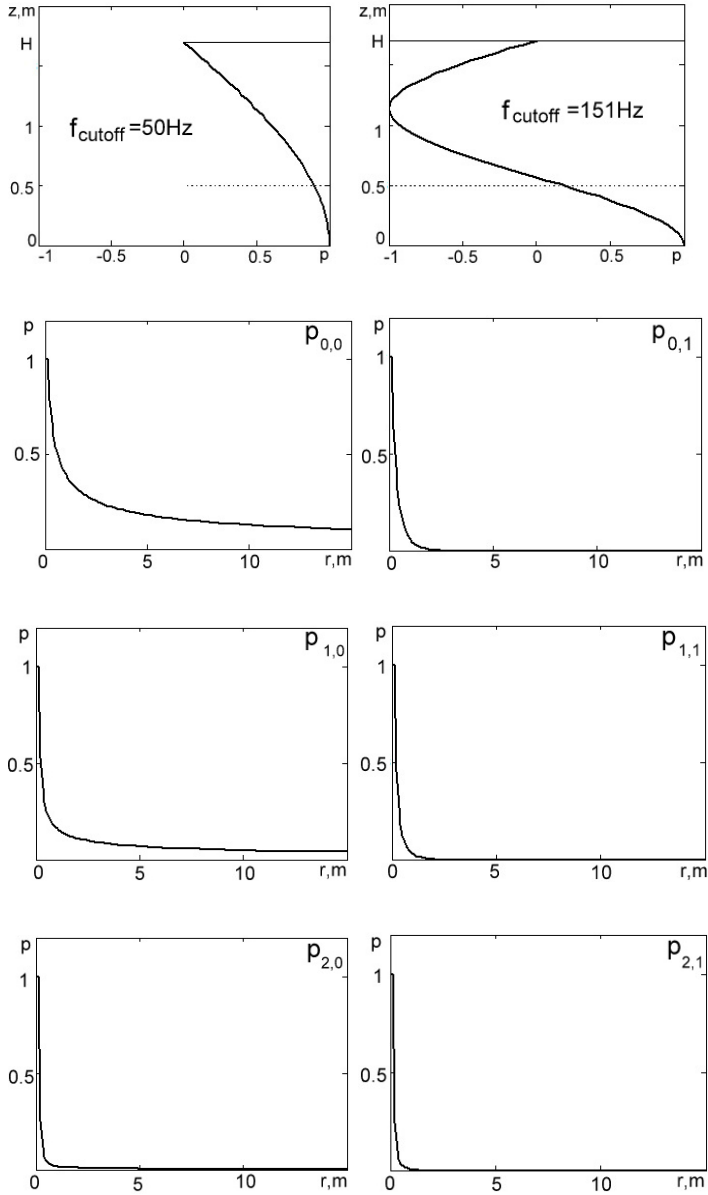
Figure 4.12: The first six modes according to eq. 4.76

5

BEM-Simulations

To verify the analytical solutions presented in Chapter 4, a computer simulation was conducted. If people in the audience are modelled as upright rigid cylinders on a rigid surface, the propagation of sound through an audience can be represented as a boundary problem and can therefore be modelled using the Boundary Elements Method (BEM). The foundations of BEM are extensively described in literature, for example in (KIRKUP, 2007). For the modelling presented in this chapter commercially available software Virtual Lab from LMS is used (*LMS Virtual Lab* n.d.) with the following simulation parameters:

Nodes and Elements:	40664 Elements and 21785 nodes
Mesh type and size:	Triangular mesh (TRI3) made of linear elements with a maximum length of 250mm
Software:	Virtual.Lab version V11-SL2
Computer:	64-bit Windows 7 PC with Intel Core i7-2600 CPU 3,4 GHz, 16 GB RAM memory, 1 core in use
Frequency range:	20-120 Hz in 1 Hz steps
Simulation:	Indirect harmonic BEM
Boundary properties:	Z=infinite (acoustical hard boundary)
Ground:	Simulated by a symmetry plane
Air absorption:	Is neglected
Source:	1 Monopole with source strength of $1kg/s^2$, which corresponds to 1 Pa at 1m distance
Medium:	Air, with c = 340 m/s
Simulation time:	21 hours

5.1 BEM-simulation layout

Three models were constructed and calculated (Fig. 5.1 - 5.3). The first two aim to verify the one-dimensional analytical solution described in 4.1 at two different concentrations of people in the audience. The third model aims to verify the analytical solution in cylindrical coordinates described in 4.4

The frequency range of the simulations was 20 - 120 Hz. The limiting factor for every simulation was the maximum number of boundary elements and the corresponding number of cylinders that the BEM-solver could handle.

The average height of the cylinders was 170 cm, the average radius 25 cm. The cylinders are placed randomly within a given audience area with a constant concentration. A point source was located at the height of 0.3 m from the floor 2 m before the audience in the first two models, in the circular model the source was located in the centre.
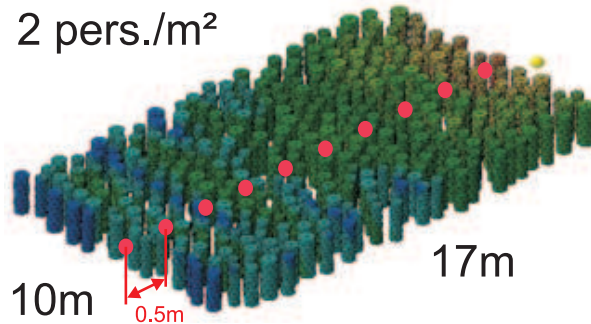

Figure 5.1: The layout of the first BEM-model. The audience occupies an area of 10x17m. The source is 2m before the audience, microphones are located on the central axis on 0.5m distance from each other.

5.2 BEM-simulation results

5.2.1 Rectangular geometry, concentration 2.6 pers./m^2

The following figures present the sound pressure level distribution within the audience and above it. Fig. 5.4 shows the sound pressure distribution on the surfaces of cylinders.
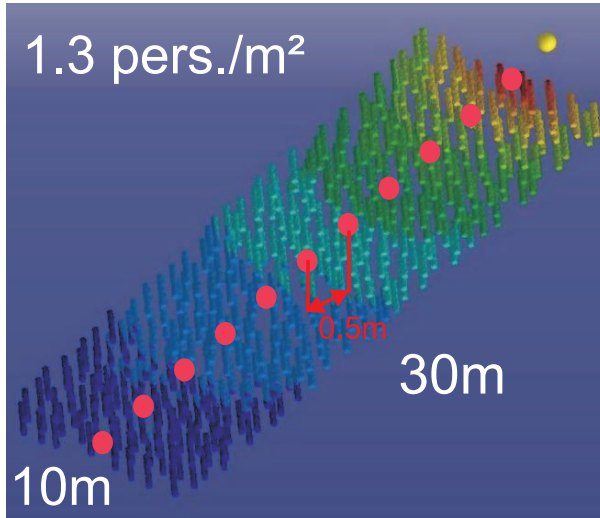
Figure 5.2: The layout of the second BEM-model. The audience occupies an area of 10x30m. The source is 2 m before the audience, microphones are located on the central axis on 0.5 m distance from each other.

Fig. 5.5 presents the sound pressure level drop over the distance within the audience and above it vs. sound pressure level drop in the absence of an audience. Below 80 Hz an interference-like picture is formed with the distance between peaks about half of the wavelength. The minimum at the rear boundary of the audience (L = 17 m) indicates a soft boundary between the audience and the air.

5.2.2 Rectangular geometry, concentration 1.3 pers./m^2

In this section the simulation results for concentration 1.3 pers./m^2 are shown. The trend is similar to 5.2.1: below 80 Hz an interference-like structure is seen, at higher frequencies the picture is distorted due to relatively large distance between receivers, but the average sound pressure level within the audience is still higher than in the free field. However, at high frequencies above the audience the sound pressure level in the free field is higher than in the presence of an audience at farther distances from the source.
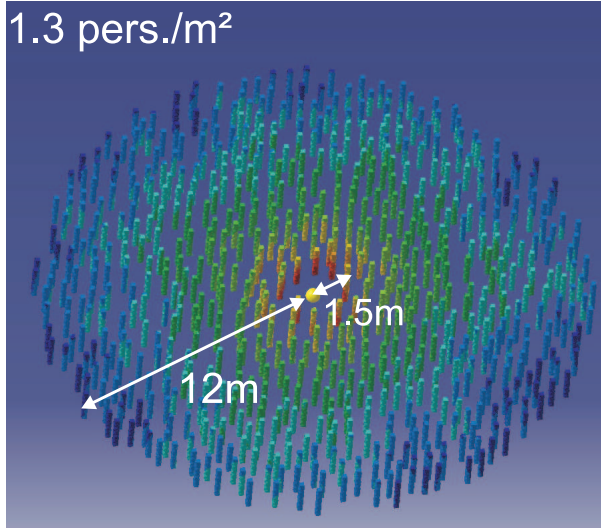
Figure 5.3: The layout of the third BEM-model. The audience occupies a ring with the inner radius of 1.5 m and the outer radius of 12 m. The source is located in the centre.

5.2.3 Circular geometry, density 2 pers./m^2

A point source was located in the centre of the circle, and the receivers in concentric circles of increasing radii (Fig. 5.7)

The sound pressure in microphones was averaged for every circle to exclude the variation over θ:

$$p(r) = \sqrt{\sum_{i=1}^{N} \frac{p_i(r)^2}{N}} \qquad (5.1)$$

A sample sound pressure distribution over r is shown in Fig. 5.8.

The sound pressure decreases with the increase of the distance and looks similar to $\frac{1}{(r)^{\frac{3}{2}}}$.
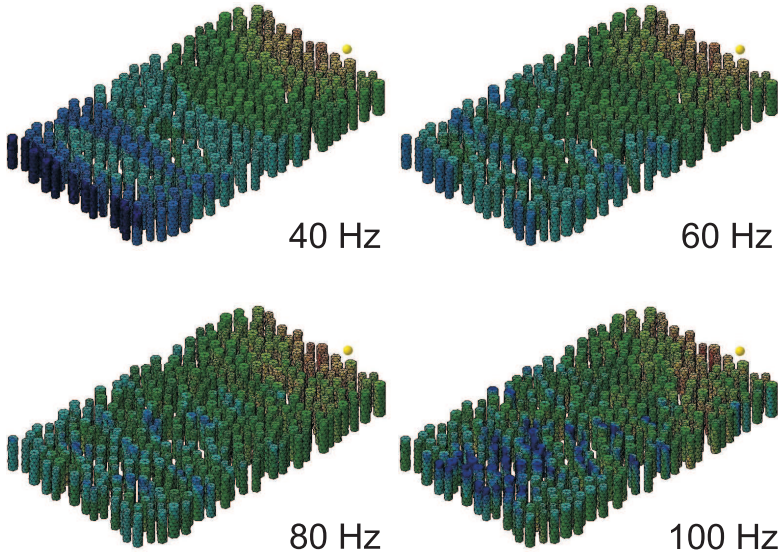
Figure 5.4: Sound pressure level distribution over the audience, concentration 2.6 pers./m^2, colour scale: 2.5 dB/division.

Let's compare the sound pressure $p(r)$ calculated according to (4.76) for the mode (0,0). The coefficients B for $H_m^{(2)}$ are assumed 0 since $H_m^{(2)}$ increases with the increase of r. Other parameters were taken as follows: $A = 1, E = 1, \theta = 0, z = 0.5m$. There are three curves on each picture: theory, simulation and asymptote, all normalized the way that they give 1 at 0.5m. In the simulation the cylinders start at $r = 1.5$ and end at $r = 10.5$.

As indicated in 4.4, the mode (0,0) has a cutoff frequency of 50 Hz. Below the cutoff frequency this mode alone is quite close to the BEM-simulation result, but above 50Hz it has less decay than the simulation. Naturally, higher order modes are needed to describe the steep decay. Fig. 5.10 represents the same curves as in Fig. 5.9, but the theoretical curve is now the sum of the first three modes: (0,0), (1,0), (2,0) with the coefficient A chosen equal to 1 for every mode. The theoretical result is now closer to the BEM-simulation than it was for the single mode (0,0).

The sound pressure distribution in a layer of audience can therefore be roughly approximated by a sum of a few cylindrical modes, calculated from the simplified

case of ideal hard and soft horizontal boundaries and no vertical boundaries of the audience. However, a correct theoretical description requires taking the impedance of an audience into account, which results in all the coefficients of eq. (4.72) being non-zero. Also, the source must be taken into account, which can be done by surrounding the source by a surface and specifying suitable boundary conditions on it (WILLIAMS, 1999).
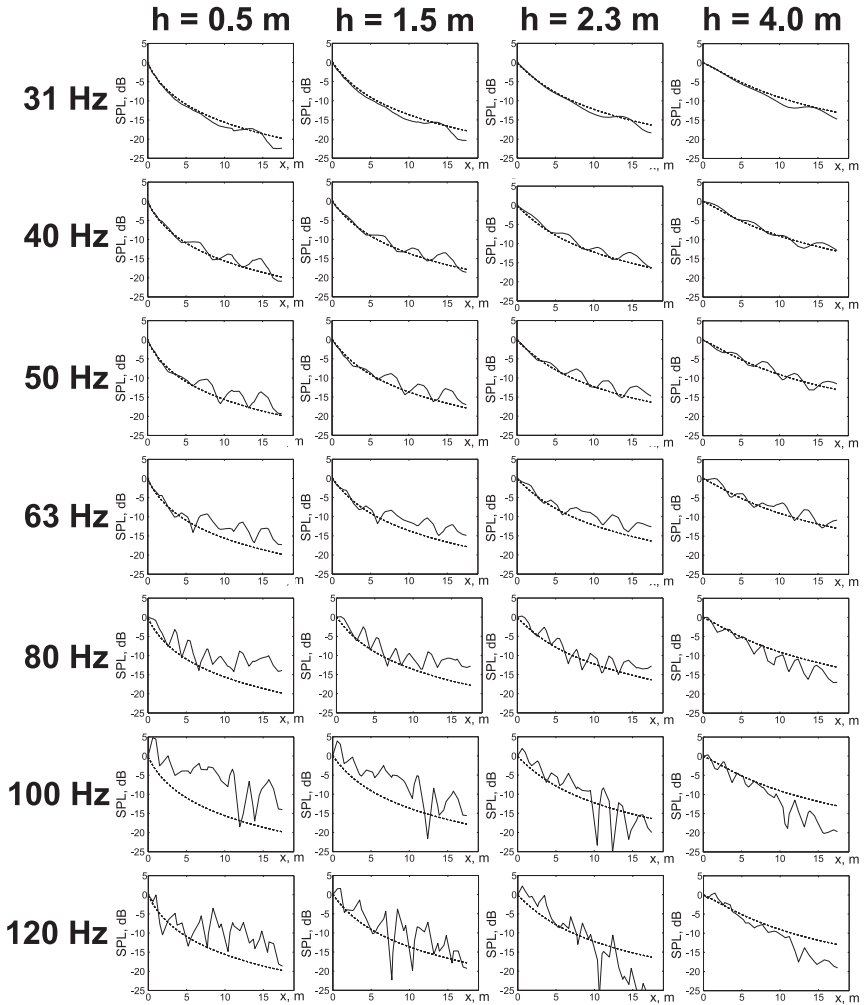
Figure 5.5: Sound pressure level distribution over distance at different heights and different frequencies with and without the audience. Solid line represents results with the audience present, dashed line - without audience
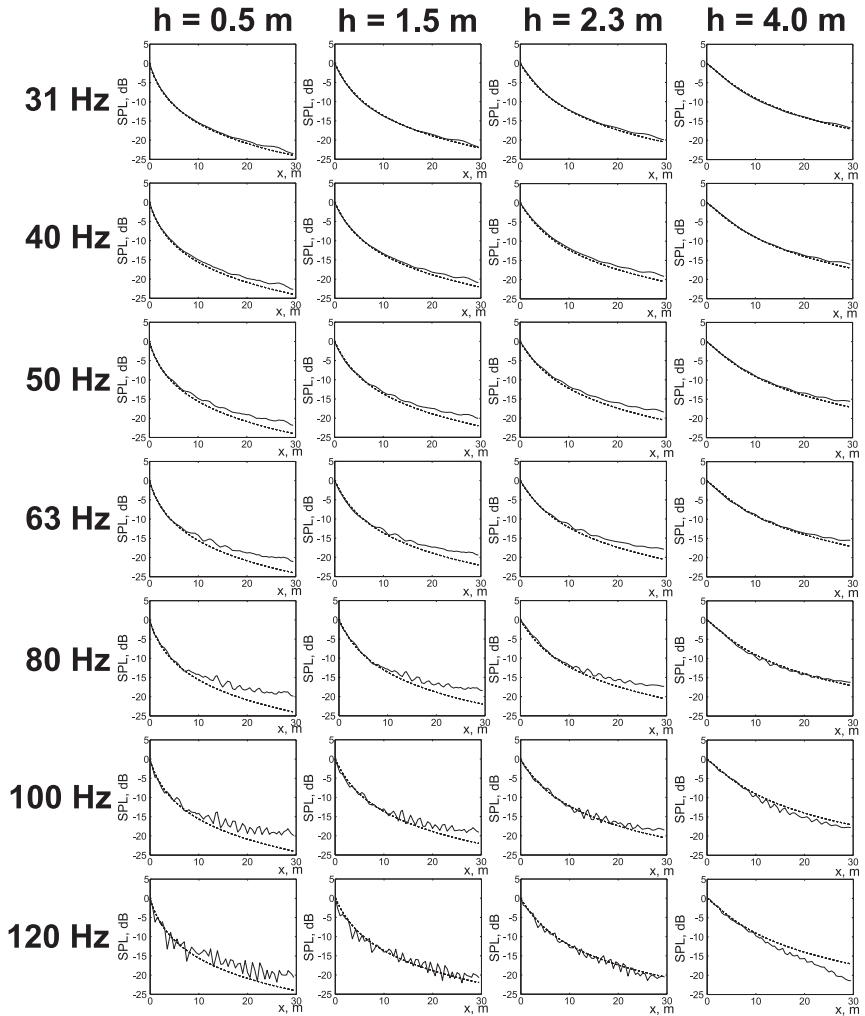
Figure 5.6: Sound pressure level distribution over distance at different heights and different frequencies with and without the audience. Solid line represents results with the audience present, dashed line - without audience
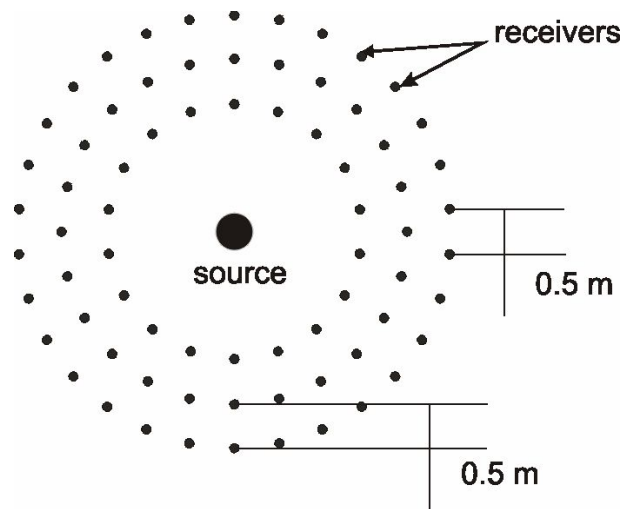
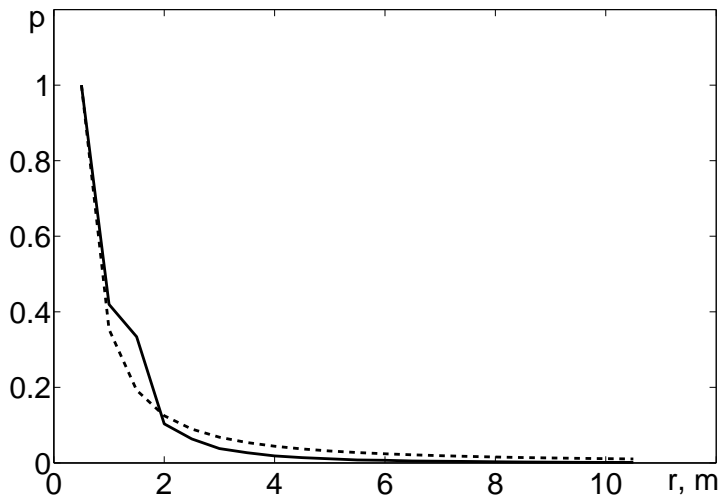**Figure 5.7:** Source and receivers' positions

Figure 5.8: Simulated sound pressure distribution over r at 30Hz. Solid line - simulated sound pressure, dashed line - asymptote $\frac{1}{(\sqrt{r})^3}$
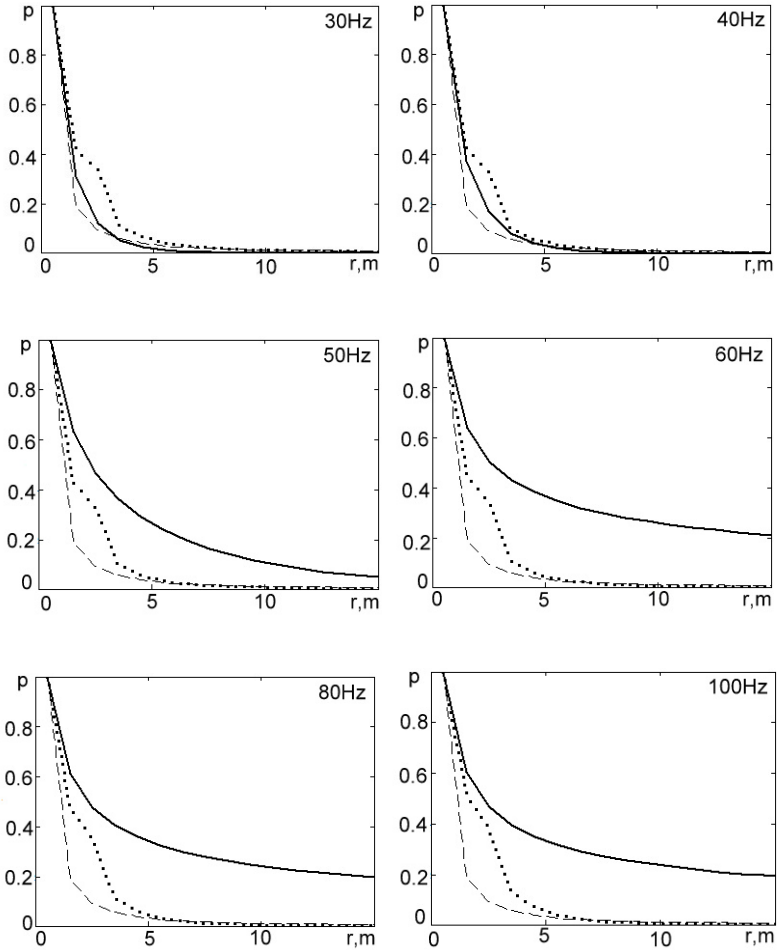
Figure 5.9: Sound pressure distribution over r at different frequencies. Solid line is theoretical value of the mode (0,0) calculated according to 4.76, dotted line is the result of the BEM-simulation and dashed line is asymptote $\frac{1}{(\sqrt{r})^3}$
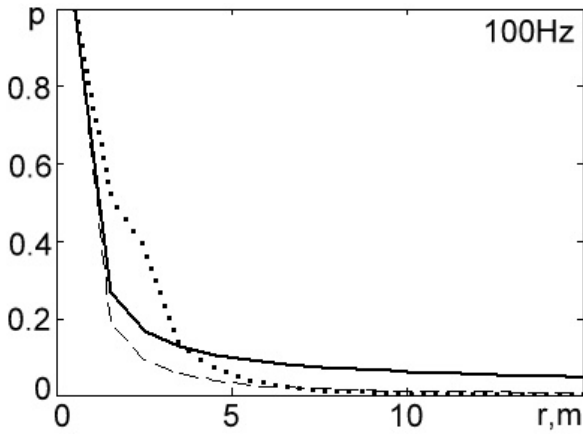
Figure 5.10: Sound pressure distribution over r at 100Hz. Solid line is the sum of the first three modes: (0,0), (1,0), (2,0), calculated according to 4.76, dotted line is the result of the BEM-simulation and dashed line is asymptote $\frac{1}{(\sqrt{r})^3}$

6

Scale measurements

To verify the results of the BEM simulations, scale model measurements were conducted. Scale modelling is a well-known technique in room acoustics that is often used for concert hall design. A room is scaled down to a reasonable size and the frequency range is scaled up accordingly. For modelling people as cylinders wood is a suitable material, almost non-absorbing and easy to handle. Cylinders were made out of conventional broom sticks of 23 mm diameter, which gave a scale factor of 21.7, given the average diameter of human body of 0.5 m. The corresponding height of the cylinders was 78 mm. The listening area of 10 x 17 m turned into an area of 46 x 78 cm and the frequency range of 30 - 120 Hz into 651 - 2604 Hz. The measurements were taken at four heights: 23 mm, 69 mm, 106 mm and 184 mm corresponding to 0.5 m, 1.5 m, 2.3 m and 4m.

6.1 Measurement setup

The scale model reproduced the layout used for the BEM-simulation described in 5.2.1, including the exact cylinders coordinates and microphones positions (Fig. 6.1 - 6.3). The influence of facial expressions of the cylinders on the sound propagation are subject to future research. A 1/4" microphone was used; 17 measurement positions were located along the central axes of the model with an average step of 23 mm in between and a little shift to allow the microphone to fit between cylinders in the same way the receivers were located in the BEM model. As a sound source a 2" loudspeaker was used as the smallest speaker still able to produce a reasonable sound pressure level in the desired frequency range.
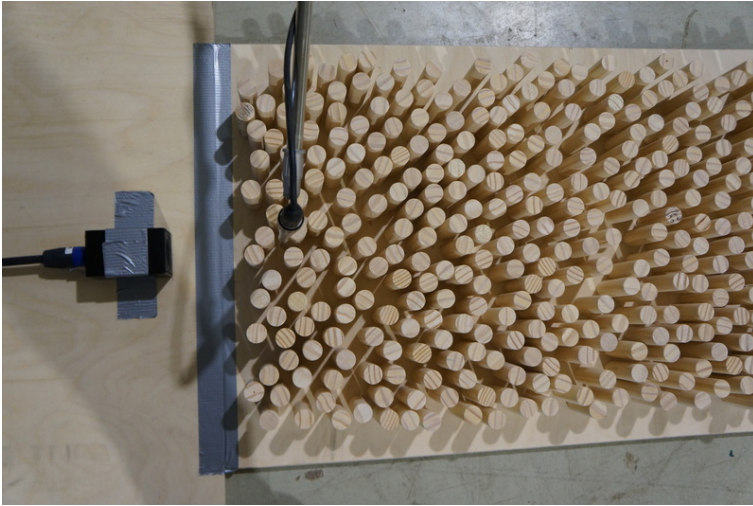
Figure 6.1: Scale model, top view

6.2 Results

Fig. 6.4 shows the summary of measurement results at different heights and frequencies. Heights and frequencies are given in the real life scale. Similar to the BEM-simulation, there is a clear interference-like picture at low frequencies that becomes less clear with the frequency increase. The amplitude of the interference gets smaller above the audience than within it.
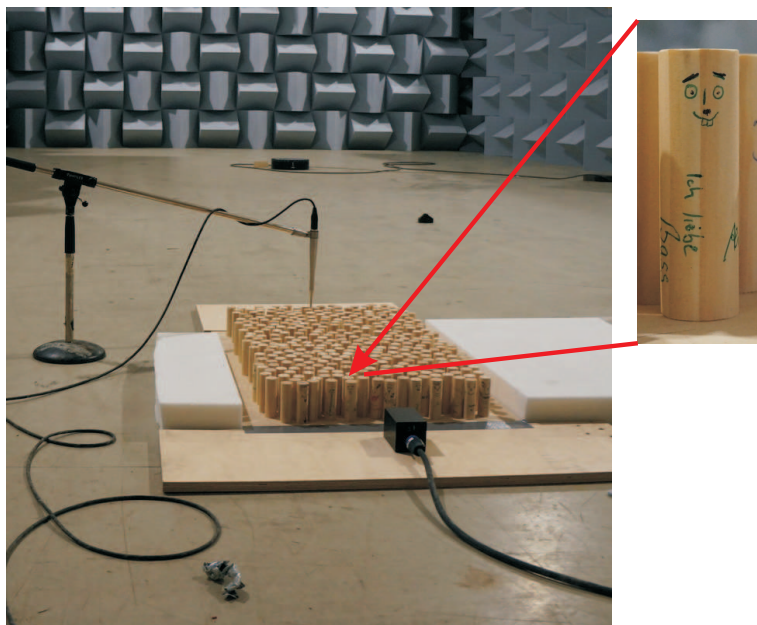
Figure 6.2: Scale model, front view
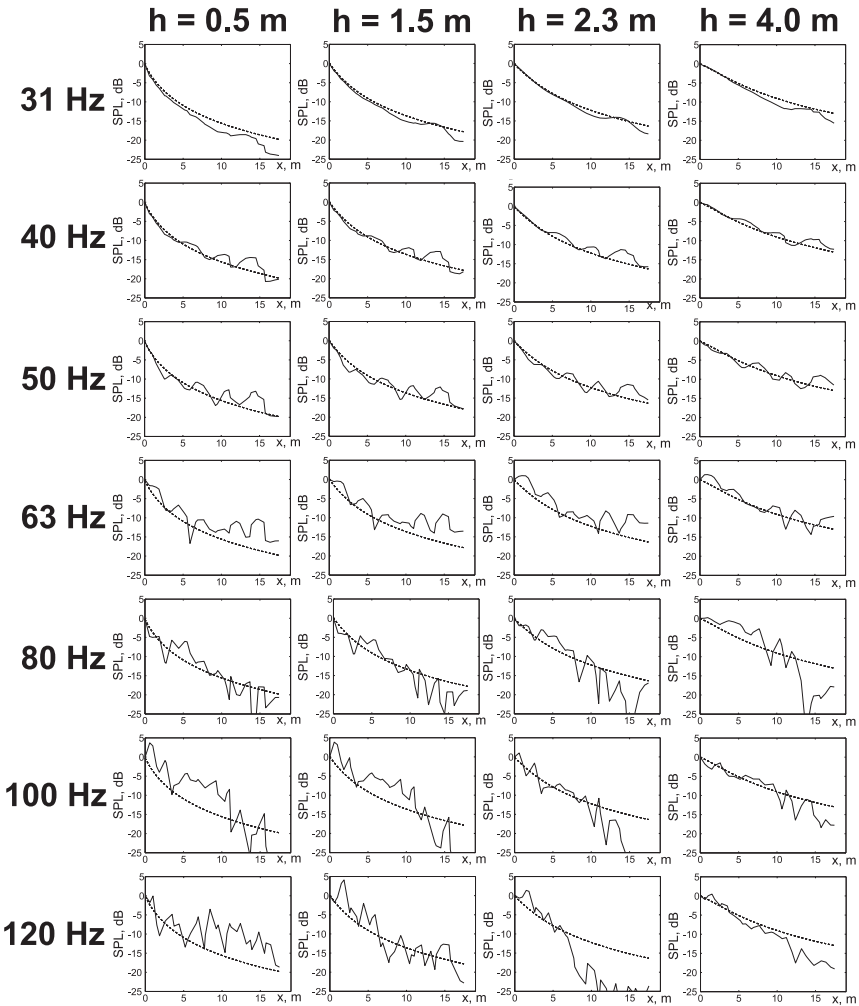

Figure 6.3: Scale model, side view

Figure 6.4: Sound pressure distribution over distance at different heights and different frequencies within or above the audience. Solid line represents results with the audience present, dashed line - ideal point source

7

Live concert measurements

7.1 Live measurement technique

To obtain the necessary experimental data, several hundreds of people have to be collected in an open space and the sound field of a powerful low frequency source has to be measured at multiple positions within the crowd. This kind of experiment is hard to organize on its own, but an environment of a large scale open-air concert or festival offers perfect measurement conditions: a large crowd is present along with powerful low frequency sound sources. The limitation is, however, that the ongoing event must not be disturbed, and the interference with the show should be minimal. The following section describes a method complying with this limitation.

7.1.1 Background

Available measurement systems can use a variety of deterministic and non-deterministic stimuli to determine the impulse response of a sound system. Typical deterministic stimuli are MLS (SCHROEDER, 1979; VORLÄNDER and KOB, 1997) or sweep (FARINA, 2000). Both MLS and sweep techniques allow fast and precise measurements of a sound system; however, both are inapplicable in a concert situation since they would disrupt the event.

Alternatively, the use of the current program signal of the system (AHNERT, FEISTEL, and FINDER, 2006; AHNERT, FEISTEL, and MIRON, 2007; J. MEYER, 1992) as measurement stimuli allows very unobtrusive measurements, although requires numerous averages to achieve an acceptable signal to noise ratio. However, measuring only one component of a sound system with this technique requires

switching off the rest of the system and running the component of interest, in our case subwoofers, alone. In a concert environment this is impossible.

The following method overcomes this limitation of the program signal measurement technique and allows to obtain the impulse response or corresponding frequency response of subwoofers without switching off the rest of the system.

In general, a concert sound system consists of two different kinds of loudspeakers. This separation into two general types of loudspeaker enclosures allows each to be specialized for its purpose, which in case of a concert sound system amongst other things is to produce its assigned frequency range at a very high level. Accordingly, there are mid and high-frequency loudspeakers, commonly termed "tops", and low-frequency loudspeakers, commonly called subwoofers or "subs" for short. Within tops and subs there may be additional diversification with regard to specific coverage angles when it comes to tops or low and very low frequencies when it comes to subs, but for this thesis, the aforementioned general differentiation shall suffice (Fig. 7.1). Both tops and subs can employ multiple sources at different positions; the frequency responses of the two groups overlap in a wide or narrow frequency band, depending on the kind of sound system used. (Fig. 7.2)
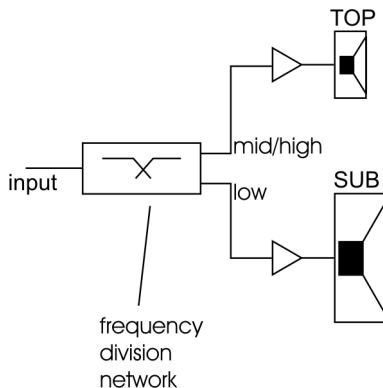

Figure 7.1: Differentiation between low and mid/high frequency loudspeakers in a concert sound system

This work focuses on extracting the frequency response of the low frequency loudspeakers, referred to as subs or subwoofers in the document.

Program signal measurement techniques were developed by several authors (AHNERT, FEISTEL, and FINDER, 2006; AHNERT, FEISTEL, and MIRON, 2007;
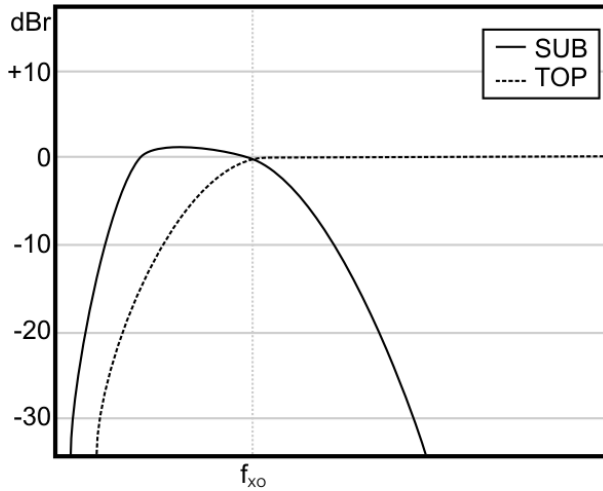
Figure 7.2: Example of frequency division and typical responses in a concert sound system

J. MEYER, 1992). The transfer function of the system under test (Fig. 7.3) is derived by dividing the measured frequency response through the input signal and the previously measured hardware reference (AHNERT, FEISTEL, and FINDER, 2006; AHNERT, FEISTEL, and MIRON, 2007) :

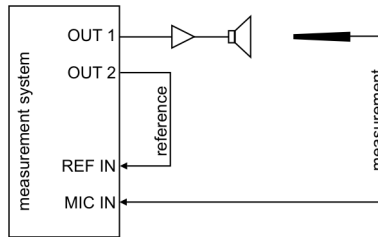$$H(\omega) = \frac{Out(\omega)}{Inp(\omega)} \tag{7.1}$$

Figure 7.3: Measurement setup for program material measurements

The impulse response of the system is described by eq. 7.1. The corresponding frequency response is

$$H_{total}(\omega) = \int (h_{tops}(t) + h_{subs}(t))e^{-i\omega t} \, \mathrm{d}t. \tag{7.2}$$

The exact forms of functions $h_{tops}(t)$ and $h_{subs}(t)$ depend on the layout of the sound system and the measurement point location, but eq. 7.2 is valid for every layout due to the linearity of the Fourier transform.

First, the impulse response of the full system is measured. For the second measurement, the component of interest - the subwoofers - is delayed by a time Δt. Then the impulse response and frequency response are

$$h_{total}^{delayed}(t) = h_{tops}(t) + h_{subs}(t - \Delta t) \tag{7.3}$$

$$H_{total}^{delayed}(\omega) = \int (h_{tops}(t) + h_{subs}(t - \Delta t))e^{-i\omega t}\mathrm{d}t \tag{7.4}$$

$$H_{total}^{delayed}(\omega) = H_{tops}(\omega)e^{-i\omega\Delta t} + H_{subs}(\omega) \tag{7.5}$$

The frequency response of the subwoofers can be calculated as follows:

$$H_{subs}^{\Delta t}(\omega) = \frac{H_{total}(\omega) - H_{total}^{delayed}}{1 - e^{-i\omega\Delta t}} \tag{7.6}$$

The denominator of eq. 7.6 turns into zero for $\omega = \frac{2\pi n}{\Delta t}, n = 0, 1...$, which causes high narrow peaks in the frequency response. The peaks can be avoided by performing two measurements with different delay times Δt_1 and Δt_2. For these measurements the peaks occur at circular frequencies $\omega_1 = \frac{2\pi n}{\Delta t_1}, n = 0, 1...$ and $\omega_2 = \frac{2\pi n}{\Delta t_2}, n = 0, 1...$ respectively. The two frequency responses can be blended together as follows:

$$H_{subs}^{blended}(\omega) = \frac{H_{subs}^{\Delta t_1}(\omega)|1 - e^{-i\omega\Delta t_1}| + H_{subs}^{\Delta t_2}(\omega)|1 - e^{-i\omega\Delta t_2}|}{|1 - e^{-i\omega\Delta t_1}| + |1 - e^{-i\omega\Delta t_2}|}, \tag{7.7}$$

where $H_{subs}^{\Delta t_1}(\omega)$ is the frequency response calculated from the measurement with the delay time Δt_1 and $H_{subs}^{\Delta t_2}(\omega)$ is calculated from the measurement with the delay time Δt_2

7.1.2 Accuracy of program signal measurements

At first, the uncertainty of program signal measurements had to be estimated. For that purpose the frequency response of the system was measured outdoors 5 times at the same position using different pieces of program material (Fig. 7.4 and 7.5). Every measurement lasted about 10s.
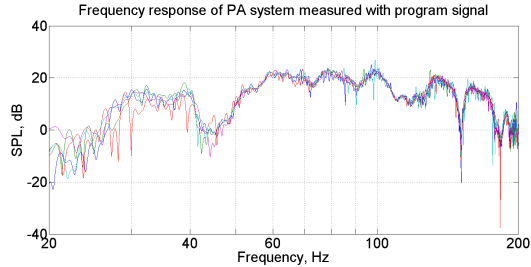

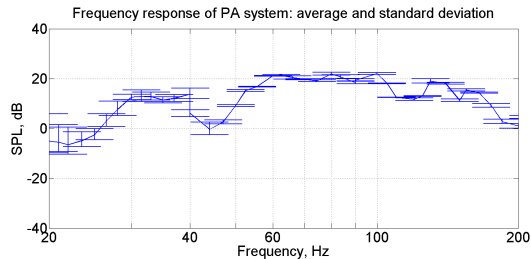**Figure 7.4:** Frequency response of a sample sound system outdoors, 5 measurements at the same position

Figure 7.5: Frequency response of a sample sound system outdoors, average and standard deviation

7.1.3 Comparison with a sweep measurement

For the Delay Method a time window of 135 ms was applied. Six delay times were used, small enough to stay unnoticed by non-experienced listeners: 2, 3, 4, 5, 6 and 7 ms. In order to study the influence of particular delay time values on the results, all combinations of delays were tested. The obtained frequency responses were then compared to the reference frequency response of the subwoofers, measured using a sine sweep.

delay1, ms	delay2, ms				
	3	4	5	6	7
2	0,725	0,523	0,437	0,436	0,427
3		0,395	0,347	0,354	0,346
4			0,292	0,312	0,315
5				0,329	0,366
6					0,615

Table 7.1: Mean squared standard deviation for different delay times combinations

First, the repeatability of the method had to be tested. To calculate the frequency response of the subwoofers three measurements of the whole system are needed: one without any delay and two measurements with two different delay values. Every measurement was repeated 5 times with different pieces of music. A 0.3 s time window was applied to the obtained impulse responses; then the desired frequency response was calculated according to the procedure described in 7.1.1 for all possible combinations of delay times. This resulted in 125 frequency responses for the chosen combination of delay time values. From this data the mean frequency response and standard deviation was calculated. This procedure was then repeated for each delay time combination (2 and 3 ms, 2 and 4 ms ... 3 and 4 ms etc.). To find the set of parameters in terms of repeatability of the results, a "mean squared standard deviation parameter" S was introduced:

$$S = \frac{\sum\limits_{i=1} \Delta_i^2}{N},\tag{7.8}$$

where i is an index over frequency, Δ_i is the standard deviation at the i-th frequency and N is the total number of frequency samples. The values of the parameter S are shown in table 7.1

The accuracy of the Delay Method is evaluated by a comparison with a reference sweep measurement. The mean and reference frequency responses are shown on Fig. 7.6; the difference between the two results is shown in Fig. 7.7 Firstly, the accuracy of program measurements according to (AHNERT, FEISTEL, and FINDER, 2006; AHNERT, FEISTEL, and MIRON, 2007; J. MEYER, 1992) is shown to be about 0.5 dB in the frequency range of 40-150 Hz (Fig. 7.5); up to 2 dB below 40 Hz and 5 dB at 20 Hz. The mean squared standard deviation parameter for the Delay Method reaches its minimum for the combination of 4 and 5 ms delays and therefore provides most repeatable results (table 7.1). For a large part of the frequency range of subwoofers, 50..90 Hz, the deviation from the reference measurement stays within 2 dB (Fig. 7.7)
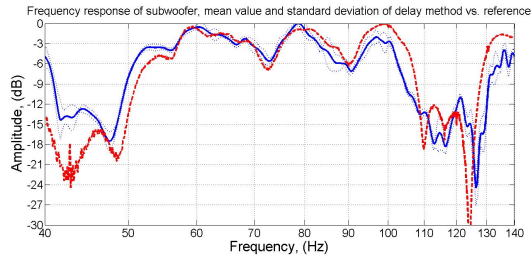
Figure 7.6: Frequency responses of subwoofers calculated according to the Difference Method and measured using a sine sweep
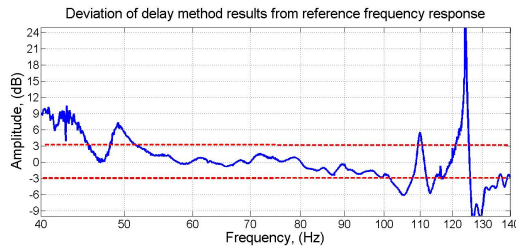

Figure 7.7: The deviation from the delay method results from the reference. Dotted lines show ± 3dB level

7.2 Discussion

The described method allows a relatively fast and unobtrusive measurement of subwoofers as a part of a complete sound system; it shows a good repeatability and correspondence with the reference measurement for the used sound systems. The Delay Method requires only a small additional time delay to the subwoofers' signal. This will cause narrow band interference effects in the transition between subs and tops which are almost unnoticeable even for an experienced listener. The Delay Method is therefore applicable for a large variety of events and allows measurements of low frequency sound propagation through an audience in a concert environment. In the following sections the results of such measurements are presented.

7.3 Live measurement setup

The first step to evaluate the influence of presence of an audience on low frequency sound propagation is to compare the sound pressure level distribution in a venue with and without audience. The easiest way is to measure the frequency response on the middle axis of the sound system at different distances from the stage, first without and then with an audience present. The typical layout for this measurement is shown in Fig. 7.8 The PA-system consists of flown arrays of broad-band loudspeakers (so-called "tops") and ground stacks or a horizontal array of subwoofers. We are interested in the signal from the subwoofers on the ground since they produce the wave going through the audience. At first measurement positions are marked on the centre line of the venue, usually with 5 m steps. Then frequency responses of the subwoofers are measured after the sound-check in the empty venue with the system already set up for the show. This reference measurement is done with sweep signals; then the frequency responses of the subwoofers are measured at the same positions several times during the show, using program material as the measurement signal (AHNERT, FEISTEL, and FINDER, 2006; SHABALINA, KAISER, and RAMUSCAK, 2010). Then the sound pressure level decay with the distance from the stage is plotted in frequency bands and compared for an empty and filled venue. As the next step the density of the audience has to be evaluated. This can be done only very roughly: at the beginning of each measurement a photograph of the audience is taken from the Front Of House-tower, then the number of people is counted manually and divided by the area (also measured before the show). During one measurement the density stays almost constant, but it changes a lot with the distance: the crowd is much denser in front of the stage and becomes sparse at the last measurement position (Fig. 7.9). However, we take the average density as a parameter.
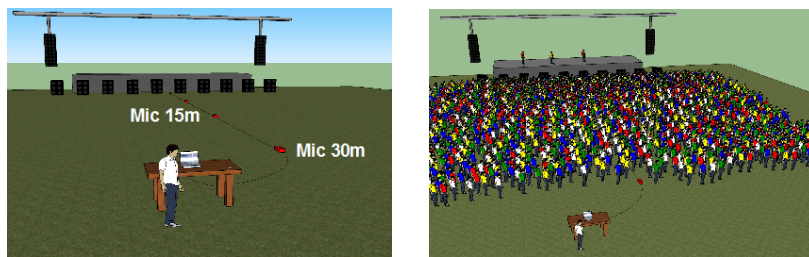

Figure 7.8: Typical layout for live measurements. Left: measurements in an empty venue, right: measurements in a full venue at the same positions

Figure 7.9: Calculation of the average density of an audience

7.4 Results for different densities

Measurements according to the above described procedure were performed at several different events several times during a concert. The average density of the crowd varied from approximately 0.3 pers./m^2 till 1.2 pers./m^2. The measurement results for the densities 0.345 pers./m^2, 0.683 pers./m^2 and 1.18 pers./m^2 are presented in the Fig. 7.10.

7.5 Discussion

The results of live concert measurements of sound propagation through an audience show a similar tendency for different densities of the audience: The decay of sound pressure level with the distance is less in the presence of audience than in free field. The effect seems to increase with the density of the crowd. However, it's very difficult to measure the effect quantitatively: a dedicated measurement session is difficult to arrange due to the large number of people to be involved, and live measurements contain large uncertainties that can hardly be eliminated. Firstly, the exact measurement positions are hard to find in the presence of the audience, the error lies within 0.5 m. Secondly, the sound engineer might change the setting of the system during the measurement (the volume of the whole system or it's component; or the frequency response by equalization) if

it is required for the show, and thirdly, the density of the crowd is not constant and hard to evaluate correctly.
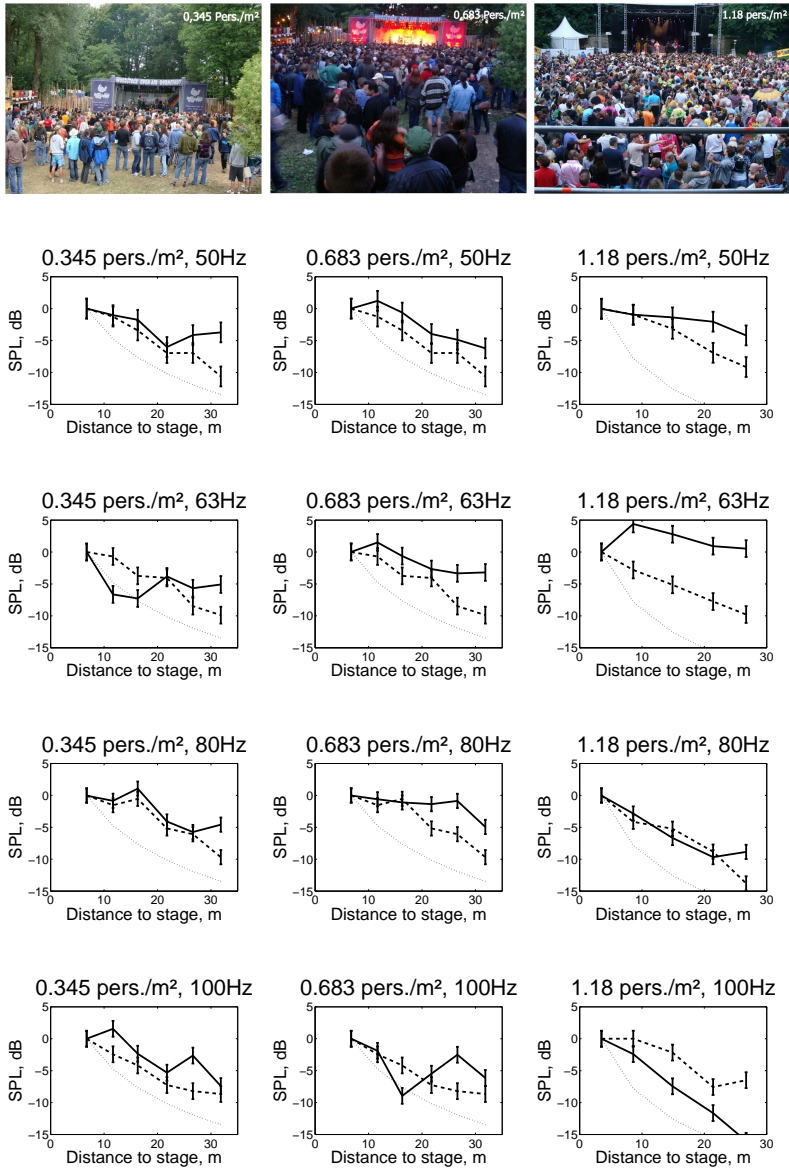
Figure 7.10: Live measurements results. Solid line - filled venue, dashed line - empty venue, dotted line - ideal point source,

8

Comparison and discussion

In this chapter the results of the investigations described in the previous chapters are compared.

8.1 BEM-simulation vs. scale measurement

The comparison between the results of the BEM-simulation, the scale measurements and a theoretical point source in a free field is presented in Fig. 8.1, where all plots are normalized to 0 dB at the first measurement point. The simulation shows a good correspondence with the scale measurements with a little more deviation above 63 Hz and a little less below. Larger deviation at higher frequencies might be caused by uncertainties of the microphone positions.

The correspondence shows that the BEM-simulation correctly predict the propagation of sound through an array of hard cylinders and can therefore be used for further investigations.

8.2 BEM-simulation vs. analytical solution

Analytical and BEM-models don't allow direct comparison since plane waves were used for the former and spherical for the latter. However, both results show interference effects (Fig. 4.6, Fig. 4.7, Fig. 5.5 and Fig. 5.6), where the distance between the peaks is half of the wavelength in the corresponding medium. It doesn't depend on the type of wave and can therefore be compared. The wavelength $\lambda = \frac{2\pi}{k}$ of the analytical model is calculated according to eq. 4.6 - 4.8 for the two given values of the concentration ν. The wavelength of the

f, Hz	λ			
	$\nu = 2.6\frac{pers.}{m^2}$		$\nu = 1.3\frac{pers.}{m^2}$	
	theory	BEM	theory	BEM
31	11.75		13.25	
40	9.11	9.5	10.27	9.1
50	7.29	7.1	8.21	7.7
63	5.78	5.4	6.52	6.2
80	4.56		5.13	
100	3.64		4.12	
120	3.04		3.42	

Table 8.1: Wavelength calculated according to the analytical model and BEM-simulations

BEM-model is estimated from the distance between peaks on the Fig. 5.5 and Fig. 5.6. This estimation is possible only at 40 Hz, 50 Hz and 63 Hz, where the interference peaks are clearly visible, and gives an uncertainty in the wavelength of $\Delta = \pm 0.5m$ due to the size of cylinders.

However, within the given uncertainty the calculated wavelengths of the BEM-models match the analytical model quite well. Also, the wavelength in a less concentrated audience is generally longer than in a concentrated audience, which corresponds to the decrease of the speed of sound with the increase of concentration shown in Fig. 4.3.

The decrease of the speed of sound in an audience in comparison to the speed of sound in the air is not obvious at the first glance: the average volume density of an audience is greater than the density of air, and in a denser medium, like, for instance, water, the speed of sound should increase. In an audience, however, the structure factor plays an important role: the wave has to "go around" the obstacles, and the greater the concentration of the obstacles, the longer is the way in comparison to the air.

8.3 Verification through live measurements

Live measurement results are hard to compare with BEM-simulation or analytical solutions: the distance of 5 m between microphone positions doesn't allow to see the interference effects, and the field of the concert subwoofers in an empty venue is far from a field of an ideal point source. However, the tendency of a

smaller decrease of the sound pressure level within an audience than in an empty venue is still present.

Fig. 8.2 and Fig. 8.3 show both a BEM-simulation result (left) and a live measurement result (right) at 50Hz and 63Hz. All the plots demonstrate a smaller decrease of the sound pressure level in the presence of audience, but the BEM-simulation result show interference dips that can't be visible in the live measurement due to the large distance between the microphone positions. Still, the live measurements need a lot of improvement to be correctly compared with the simulation.
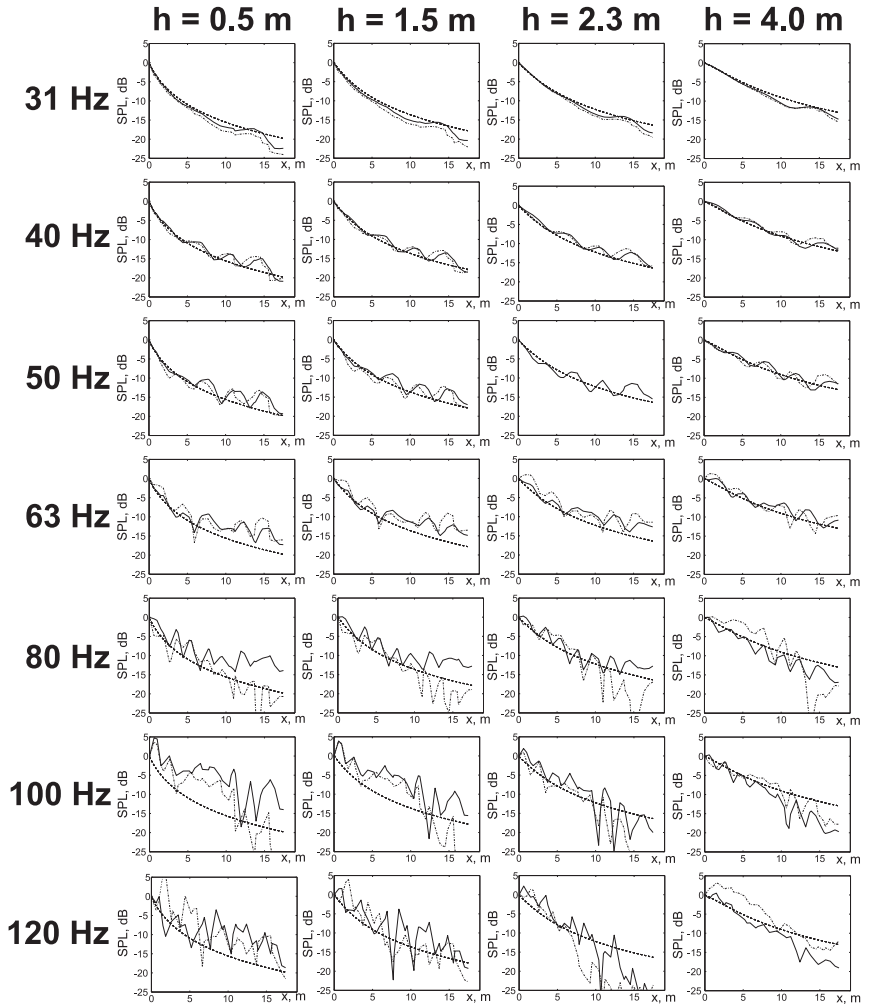
Figure 8.1: Sound pressure distribution over distance at different heights and different frequencies with and without the audience. Solid line represents results of the BEM-simulation, point-dash line is the results of scale model measurements, and dashed line is a point source - without audience
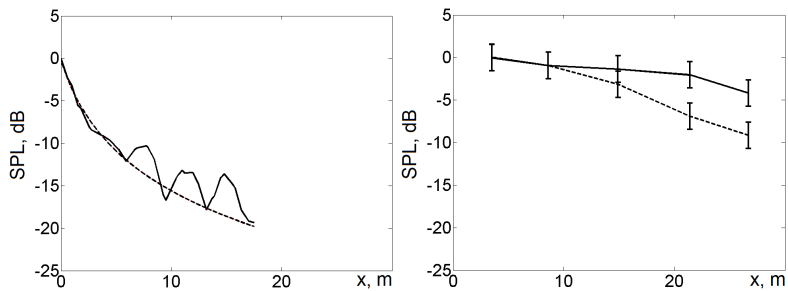
Figure 8.2: BEM-simulation (left) and live measurements results at 50 Hz. Solid line - filled venue, dashed line - empty venue
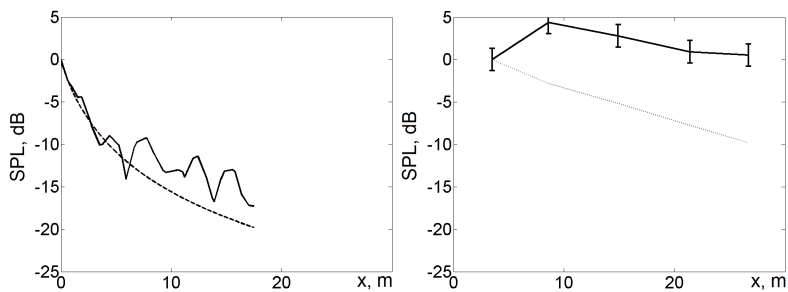

Figure 8.3: BEM-simulation (left) and live measurements results at 63 Hz. Solid line - filled venue, dashed line - empty venue

9   ———————————————————

Conclusions and outlook

This thesis presents an investigation on how low frequency sound propagates through an audience. New experimental data of diffuse field absorption of the human body at low frequencies was obtained and shown to be from 0.025 to 0.07 m^2 per person in the frequency range from 30 to 100 Hz.

It was experimentally shown that there is a measurable difference between the sound pressure level distribution in an empty venue and in the presence of audience, the sound pressure level decay with the distance tends to be less in the presence of audience.

A new live measurement method was developed to evaluate the low frequency sound pressure level distribution in an occupied venue without disturbing the ongoing event.

It was shown that with the use of porous medium theory an audience can be modelled as an equivalent fluid, which parameters depend only on the concentration of the audience, both for a constant and a variable concentration of people. The modelling results correspond to the BEM-modelling of an audience as a set of hard cylinders. This approach supplements the conventional model of a audience as a surface absorber for mid- and high frequencies and extends it into low frequencies and non-diffuse fields.

It was shown both analytically and with the use of BEM-simulation that the finite height of an audience leads to a modal field within an audience as well as to evanescent waves under a cutoff frequency.

It can be concluded that at low frequencies an audience forms a medium with its impedance significantly different from the impedance of the air, which leads

to the reflection of sound waves from the boundaries back into the audience and therefore the increase of the sound pressure level. The wave number, speed of sound and impedance appeared to be real, however, a small complex part might appear if the small diffuse field absorption of the human body is taken into account.

For future research more controlled measurements with large audiences are needed, along with a further investigation of an audience as a layer on a rigid surface. For the latter the finite horizontal dimensions of an audience have to be taken into account. The equivalent fluid model has to be verified by a Finite Element Method simulation. An application of a multiple scattering theory might be insightful as well, as it should give the same results as the equivalent fluid model, connecting therefore microscopic and macroscopic parameters of an audience. The application of the porous material theory to an audience must be extended to the oblique wave incidence.

Possible applications of the findings are mostly sound system design or event planning: knowing the influence of an audience of given concentration on the sound pressure level distribution, one can find a better placement of subwoofers and listener areas, along with optimal concentrations of listeners for every zone of the listening area. Decrease of the concentration from the front to the back of an audience can, for example, prevent reflections from the back and eliminate interference peaks. Information about the layer modes and propagating and evanescent waves can help to create a better frequency correction or equalisation of the subwoofers.

Bibliography

W. Ahnert, S. Feistel, and E. Finder (2006). "Software Based Live Sound Measurements." In: *Audio Engineering Society Convention 121*, Preprint 6988.

W. Ahnert, S. Feistel, and A. R. Miron (2007). "Software-Based Live Sound Measurements, Part 2." In: *Audio Engineering Society Convention 123*, Preprint 7304.

Y. Ando and M. Takaishi (1982). "Calculations of the sound transmission over theater seats and methods for its improvement in the low frequency range." In: *The Journal of the Acoustical Society of America* 72.August, pp. 443–448.

K. Attenborough (1982). "Acoustical characteristics of porous materials." In: *Physics Reports*.

L. Beranek (1960). "Audience and seat absorption in large halls." In: *The Journal of the Acoustical Society of America* 32.1958, pp. 465–468.

L. M. Brekhovskikh and O. A. Godin (1989). *Akustika sloistykh sred*. Nauka, Moskva.

T. F. W. Embleton (1966). "Scattering by an Array of Cylinders as a Function of Surface Impedance." In: *The Journal of the Acoustical Society of America* 40, pp. 667–670.

A. Farina (2000). "Simultaneous measurement of impulse response and distortion with a swept-sine technique." In: *Audio Engineering Society Convention 108*, Preprint 5093.

L. Foldy (1945). "The multiple scattering of waves." In: *Physical Review* 67.3-4.

A. Ishimaru (1999). *Wave propagation and scattering in random media*.

U. Kath and W. Kuhl (1964). "Messungen zur Schallabsorption von Personen auf ungepolsterten Stühlen." In: *Acustica* 14.

S. Kirkup (2007). *The Boundary Element Method for Acoustics*.

D. Kunstmann (1967). "Modellenuntersuchungen zur Schallausbreitung über Publikum (Schallstreuung an Kugelzeilen)." In: *Acustica* 18, p. 259.

H. Kuttruff, E. Meyer, and F. Schulte (1965). "Versuche zur Schallausbreitung über Publikum." In: *Acustica* 15, p. 175.

M. Lax (1951). "Multiple Scattering of Waves." In: *Reviews of Modern Physics* 23.5.

M. Lax (1952). "Multiple scattering of waves. II. The effective field in dense systems." In: *Physical Review* 85.1950.

LMS Virtual Lab (n.d.). `http://www.lmsintl.com/virtuallab`.

P. A. Martin (2006). *Multiple scattering: interaction of time-harmonic waves with N obstacles*. Cambridge University Press.

F. P. Mechel (1966). "Die Streuung ebener Wellen an Zylindern und Kugeln komplexer Impedanz." PhD thesis. Universität Göttingen.

F. P. Mechel (1989). *Schallabsorber Bd.1. Äussere Schallfelder - Wechselwirkungen*. S. Hirzel Verlag, Stuttgart.

F. P. Mechel (1995). *Schallabsorber Bd.2. Innere Schallfelder - Strukturen*. S. Hirzel Verlag, Stuttgart.

F. P. Mechel (1998). *Schallabsorber Bd. 3. Anwendungen*. S. Hirzel Verlag, Stuttgart.

E. Meyer, D. Kunstmann, and H. Kuttruff (1964). "Über einige Messungen zur Schallabsorption von Publikum." In: *Acustica* 14, pp. 119–124.

J. Meyer (1992). "Precision transfer function measurements using program material as the excitation signal." In: *Audio Engineering Society 11th International Conference: Test & Measurement*, pages.

P. M. Morse and K. U. Ingard (1968). *Theoretical Acoustics*. Vol. 36. 2. Princeton University Press, p. 927.

M. Möser (2009). *Egineering Acoustics*. Springer.

N. Nishihara, T. Hidaka, and L. Beranek (2001). "Mechanism of sound absorption by seated audience in halls." In: *The Journal of the Acoustical Society of America* 110.5, p. 2398.

I. Perez-Arjona and V. J. Sanchez-Morcillo (2006). "Nondiffractive sonic crystals." In: *Arxiv preprint physics/*. arXiv: `0606018v1 [arXiv:physics]`.

I. Pérez-Arjona, V. Sánchez-Morcillo, J. Redondo, V. Espinosa, and K. Staliunas (Jan. 2007). "Theoretical prediction of the nondiffractive propagation of sonic waves through periodic acoustic media." In: *Physical Review B* 75.1, pp. 1–7.

M. A. Price, K. Attenborough, and N. W. Heap (1988). "Sound attenuation through trees: measurements and models." In: *The Journal of the Acoustical . . .* 84.November, pp. 1836–1844.

M. R. Schroeder (1979). "Integrated impulse method measuring sound decay without using impulses." In: *The Journal of the Acoustical Society of America* 66.2, pp. 497–500.

E. Shabalina, M. Kaiser, and J. Ramuscak (2010). "Live measurements of ground-stacked subwoofers' performance." In: *Audio Engineering Society Convention 128*, pp. 1–6.

A. B. Shvartsburg and N. S. Erokhin (1960). "Gradientnye akusticheskie barjery (tochno reshaemye modeli)." In: *Uspekhi fizicheskikh nauk* 181.6.

V. Twersky (1962a). "On Scattering of Waves by Random Distributions. I. Free-Space Scatterer Formalism." In: *Journal of Mathematical Physics* 3.4, p. 700.

V. Twersky (1962b). "On Scattering of Waves by Random Distributions. II. Two-Space Scatterer Formalism." In: *Journal of Mathematical Physics* 3.4, p. 700.

V. Twersky (1966). *Multiple scattering of waves by a volume distribution of parallel cylinders.* Vol. 19. October 1953.

M. Vorländer and M. Kob (1997). "Practical aspects of MLS measurements in building acoustics." In: *Applied Acoustics* 52.3-4, pp. 239–258.

D. de Vries and M. M. Boone (2006). *Sound control part 1.*

E. G. Williams (1999). *Fourier Acoustics: Sound Radiation and Nearfield Acoustical Holography.* Academic Press, p. 306.

C. Zwikker and K. W. Kosten (1949). *Sound absorbing meterials.* Elsevier.

Acknowledgements

Curriculum Vitae

Personal Data

	Elena Shabalina
24. 11. 1984	born in Ryazan, Russia

Education

1991 – 2001	52. Luceum, Ryazan, Russia

Higher Education

09/2001 – 01/2007	Diploma Degree in Radiophysics and Physical Electronics at Moscow State University Focus: Physical Acoustics

Professional Experience

10/2012 – now	R&D Acoustics at d&b audiotechnik GmbH, Backnang, Germany
12/2008 – 07/2012	Researcher at the Institute of Technical Acoustics (ITA), RWTH Aachen University, Aachen, Germany
09/2008 – 10/2012	Lecturer in Acoustics and Sound System Design at the Insitute of Cinematography, Moscow, Russia
09/2007 – 09/2008	Lecturer in Physics, Mathematics and Acoustics at the Gnesins Academy of Music, Moscow, Russia
12/2005 – 03/2008	Acoustician at Aris-Pro, Moscow, Russia
08/2004 – 02/2012	freelance acoustic consultant

Backnang, Germany, December 20, 2013